# Excitation of Isobaric Analog States in Medium-Weight Nuclei by the $(d,p)$ Reaction at 28 MeV*†

R. SHERR, B. F. BAYMAN,‡ AND E. ROST
*Palmer Physical Laboratory, Princeton University, Princeton, New Jersey*

AND

M. E. RICKEY AND C. G. HOOT‡
*Department of Physics, University of Colorado, Boulder, Colorado*

(Received 8 April 1965)

States of spin $\frac{7}{2}^-$ in $Ti^{47}$, $Ti^{49}$, $Cr^{51}$, $Fe^{53}$, $Fe^{55}$, $Fe^{57}$, $Ni^{57}$, $Ni^{59}$, and $Ni^{61}$ were observed by means of the $(p,d)$ reaction with 28-MeV incident protons. In each case the highest $\frac{7}{2}^-$ state seen was found to be the isobaric analog of the lowest $\frac{7}{2}^-$ state of the isobar with one more neutron. Coulomb displacement energies were obtained which are in excellent agreement with known values in this mass region. The lower $\frac{7}{2}^-$ states were interpreted as "configuration states," that is, states associated with the same configuration as the analog, but with isospin lower by unity. The angular distributions in all cases were in good agreement with distorted-wave calculations. Comparison of the spectroscopic factors for the analog and configuration states with the predictions of $j$-$j$-coupling sum rules revealed that the normal procedures used in distorted-wave calculations predict too large a $Q$ dependence. However, by using radial wave functions for the picked-up neutron that are identical for all $1f_{7/2}$ states in a given nucleus, reasonable agreement with the sum rules was obtained. Reasonable agreement was also found with the strengths for various states computed from $1f_{7/2}$ shell-model calculations. The energy splitting between the analog state and the strength-weighted mean of the configuration states was also found to be in agreement with theoretical estimates.

## I. INTRODUCTION

IT has been well known for many years that isobaric (isotopic) spin is a fairly good quantum number for low-lying states of light nuclei ($A \lesssim 54$). By 1940 there was extensive information on the mirror nuclei such as $C^{13}$ and $N^{13}$ for which $T=\frac{1}{2}$ and $T_z=\frac{1}{2}(N-Z)=\pm\frac{1}{2}$. The atomic masses of these pairs differ only by the difference in the Coulomb interaction energies of the two nuclei minus the neutron-proton mass difference. Since 1950, extensive work has been done on the $T=1$ multiplets (such as $C^{14}-N^{14*}-O^{14}$), up to $A=54$. The masses of these members of $T=\frac{1}{2}$ and $T=1$ multiplets have yielded accurate empirical Coulomb-energy differences up to $Z=27$. However, for heavy nuclei or for states of high excitation, the purity of isospin has been open to question.[1,2]

Interest in isospin multiplets has been greatly stimulated by recent experiments on medium-heavy nuclei in which isobaric states at high excitation have been observed with experimental widths which suggest a high degree of isospin purity. In 1961, Anderson and Wong[3] found a state in $Cr^{51}$ at 6.5 MeV which was strongly excited in the $(p,n)$ reaction on $V^{51}$. They interpreted this state as the isobaric analog of the ground state of the target nucleus. Subsequently, Anderson and his co-workers extended this work to many elements including the rare earths.[4] Because of the limited resolution of their experiments, they were only able to set an upper limit of 100 keV to the width of the isobaric analog states, a value in reasonable agreement with estimates by Lane and Soper.[2]

In the past year, another mode of investigation of these analogue states has emerged in the work of Fox, Moore, and Robson.[5] They observed a number of compound states in the elastic scattering of protons by $Sr^{88}$ which they identified as the isobaric analogs of states of $Sr^{89}$ in the compound nucleus $Y^{89}$. Similar results were obtained for other targets.[6] From the details of the resonances, they could determine the angular momenta of the proton partial waves responsible for the resonances; these in fact corresponded to the orbital angular-momentum transfer observed in $(d,p)$ reactions on the same targets. The experimental widths of the analog states were of the order of 20 keV. Lee, Marinov, and Schiffer[7] reported more detailed measurements of this type on states of $Cu^{65}$ reached by $Ni^{64}+p$ scattering. They found proton widths in very good agreement with that expected from experimentally observed $(d,p)$ stripping on $Ni^{64}$.

* Work done under the U. S. Atomic Energy Commission, Contract AT(11-1)-535 (University of Colorado) and Contract AT(30-1)-937 (Princeton University).

† Preliminary accounts of these results were presented at the Chicago Symposium on Nuclear Spectroscopy with Direct Reactions (Proceedings ANL-6878, March 1964) and at the Washington Meeting of the American Physical Society, Bull. Am. Phys. Soc. **9**, 458 (1964).

‡ Present address: Department of Physics, University of Minnesota, Minneapolis, Minnesota.

[1] W. M. MacDonald, Phys. Rev. **100**, 51 (1955); **101**, 271 (1956).

[2] A. M. Lane and J. M. Soper, Nucl. Phys. **37**, 663 (1962).

[3] J. D. Anderson and C. Wong, Phys. Rev. Letters **7**, 250 (1961).

[4] J. D. Anderson, C. Wong, and J. W. McClure, Phys. Rev. **129**, 2718 (1963).

[5] J. D. Fox, C. F. Moore, and D. Robson, Phys. Rev. Letters **12**, 198 (1964).

[6] D. Robson, J. D. Fox, J. A. Becker, C. F. Moore, P. Richard, D. Long, S. I. Hayakawa, C. Vourvopoulos, and C. E. Watson, Tandem Accelerator Laboratory (Florida State University), Tech. Rept. No. 6, January 1964).

[7] L. L. Lee, Jr., A. Marinov, and J. P. Schiffer, Phys. Letters **8**, 352 (1964).

The present investigation of analog states using the $(p,d)$ reaction was stimulated by the above experiments and by the availability of the 28-MeV proton beam of the new Univeristy of Colorado cyclotron. The importance of observing isobaric analog states in pickup, stripping, and resonance reactions in this mass region was emphasized by French and Macfarlane[8] in 1961. They also derived sum rules for the relevant spectroscopic factors. In the $(p,d)$ reaction on a target $(Z,N)$ with ground-state isospin $T_0$, one can reach final states in the residual nucleus $(Z, N-1)$ with $T=T_0\pm\frac{1}{2}$. The final states with $T=T_0+\frac{1}{2}$ will be the analog of the low-lying states of the nucleus $(Z-1, N)$ differing from the target by one proton. In the past, successful observations of analog states by this reaction have been carried out with 18-MeV protons on some light nuclei[9] where in special cases the $T_0+\frac{1}{2}$ states are at low excitation, as for example in $N^{14}$. In even-even light nuclei the isobaric analog states lie at excitation energies of the order of 10 MeV, and for $T_0+\frac{1}{2}$ states which can be reached by the $(p,d)$ reaction in the region of $A=50$, the excitation energies are also large. For both groups of nuclei the $Q$ values are typically $-15$ to $-20$ MeV.

The $(p,d)$ reaction yields somewhat different information about analog states than the $(p,n)$ reaction or the proton-resonance experiments. In the $(p,d)$ reaction both $T_0-\frac{1}{2}$ and $T_0+\frac{1}{2}$ states are appreciably excited. States which are strongly excited are those resulting from the direct pickup of a neutron unaccompanied by configuration rearrangement. Therefore, this reaction is particularly suitable for shell-model investigation.

The $(p,n)$ reaction, on the other hand, yields the analog of the target ground state by means of a coherent charge-exchange force which may be expressed in optical-model terms.[10] This state is excited much more strongly than any other direct $(p,n)$ level. Thus this reaction has been primarily exploited from the extraction of the Coulomb displacement energy (given by the $Q$ value) and the symmetry-energy term in the optical model.

The proton-resonance experiments[5] can be carried out with very high resolution and are ideally suited for the detailed study of the structure of the $T_0+\frac{1}{2}$ states. This technique can be applied only when the Coulomb displacement energy is greater than the neutron binding energy. This limits the experiment to heavy nuclei $(A\gtrsim 90)$ except for certain special cases. In addition, the proton-resonance experiment does not investigate the low-lying $T_0-\frac{1}{2}$ levels.

Therefore, it is seen that the $(p,d)$ reaction has the special property of allowing simultaneous investigation of the analog $T_0+\frac{1}{2}$ states along with low-lying $T_0-\frac{1}{2}$ states which have the same configuration. Both kinds of states were observed in the present measurements using 28-MeV protons on targets of $Ti^{48}$, $Ti^{50}$, $Cr^{52}$, $Fe^{54}$, $Fe^{56}$, $Fe^{58}$, $Ni^{58}$, $Ni^{60}$, and $Ni^{62}$. Sections II and III which follow describe the experimental procedure and the experimental results for the individual targets. Section IV presents the discussion of our results and comparison with theory for states excited by pickup of an $f_{7/2}$ neutron. In Sec. IVA the Coulomb displacement energies obtained from the excitation energies of the $T_0+\frac{1}{2}$ states are given. Section IVB discusses the spectroscopic factors obtained through distorted-wave calculations and compares them with the sum rules of French and Macfarlane.[8] Individual spectroscopic factors for those nuclei for which $N$ and $Z$ are less than 28 are compared in Sec. IVC with predictions based on the $f_{7/2}$ shell-model wave functions of McCullen, Bayman, and Zamick.[11] In Sec. IVD, the energy difference between the $T_0+\frac{1}{2}$ and $T_0-\frac{1}{2}$ states ($T$ splitting) is discussed.

## II. EXPERIMENTAL PROCEDURE

Data were taken using the 28-MeV proton beam of the University of Colorado 52-in. sector-focused cyclotron.[12] The beam entered a 36-in. scattering chamber through a $\frac{1}{8}$-in.-diam collimator followed by a $\frac{3}{16}$-in.-diam antiscattering baffle. Deuterons from the targets were detected in a three-counter telescope using totally depleted Ortec silicon surface barrier detectors in transmission mounts. The first detector (I), 200 $\mu$ thick, provided a $\Delta E$ signal. The second detector (II) was 2000 $\mu$ thick which was sufficient to stop the highest energy deuterons encountered. The third detector (III), 350 $\mu$ thick, provided an anticoincidence signal to reject events associated with long-range protons.

The $\Delta E$ and $E$ detectors were mounted in an insulated holder and grounded through a 5-M$\Omega$ resistor. This permitted extraction of a sum signal from the two detectors in addition to the individual signals. The sum signal, a measure of the full deuteron energy, was amplified in a Tennelec, Model 100A, preamplifier. This pulse was fed to the internal amplifier of a Nuclear Data Corporation Model 160 pulse-height analyzer operated in the single parameter mode and gated by coincidence requirements described below.

Particle identification was accomplished by multiplication of $\Delta E$ and sum pulses with a field-effect transistor multiplier.[13] Alignment was optimized by two-dimensional analysis of energy and multiplier signals in the ND-160 analyzer. Since short-range particles stopping in the $\Delta E$ detector were accompanied

[8] J. B. French, Nucl. Phys. **26**, 161 (1961); J. B. French and M. H. Macfarlane, *ibid.* **26**, 168 (1961).
[9] K. G. Standing, Phys. Rev. **101**, 152 (1956); E. F. Bennett, *ibid.* **122**, 595 (1961).
[10] A. M. Lane, Phys. Rev. Letters **8**, 171 (1962).
[11] J. D. McCullen, B. F. Bayman, and L. Zamick, Phys. Rev. **134**, B515 (1964).
[12] D. A. Lind, J. J. Kraushaar, M. E. Rickey, and R. Smythe, Nucl. Instr. Methods **18–19**, 62 (1962).
[13] G. L. Miller and V. Radeka, I.E.E.E. Trans. Nucl. Sci. (to be published); see also Brookhaven National Laboratory Report No. 7448 (unpublished).

TABLE I. Summary of states seen in the present experiment. The values of $l$ are listed in column 3 and the $J^\pi$ assignments are given in column 4. Previous assignments and references are shown in the last two columns. Checks ($\surd$) in column 4 indicate consistency of the present results with previous assignments. An asterisk (*) refers to unresolved multiple peaks.

| $E_x$ (MeV) | $-Q$ (MeV) | $l$ | $J^\pi$ present | $J^\pi$ previous | Ref. |
|---|---|---|---|---|---|
| | | $Ti^{48}(p,d)Ti^{47}$ | | | |
| 0 | 9.39 | ... | ... | $\frac{5}{2}^-$ | 16 |
| 0.16 | 9.55 | 3 | $\frac{7}{2}^-$ | $\frac{7}{2}^-$ | 16 |
| 1.55 | 10.94 | 1 | $\surd$ | $\frac{3}{2}^-$ | 16 |
| 1.81 | 11.20 | (1 and 2) | $\surd$ | $(\frac{3}{2}^-, \frac{3}{2}^+)$ | 16 |
| 2.15 | 11.54 | (1) | ... | ... | |
| 2.34 | 11.73 | 0 | $\surd$ | $\frac{1}{2}^+$ | 16 |
| 2.56 | 11.95 | ... | ... | ... | |
| 2.81 | 12.20 | ... | ... | $(\frac{3}{2}^-, \frac{7}{2}^-)$ | 16 |
| 3.18 | 12.57 | 3 | $\frac{7}{2}^-$ | ... | |
| (3.84)* | (13.23) | ... | ... | ... | |
| (4.30)* | (13.69) | ... | ... | ... | |
| 7.30 | 16.69 | 3 | $\frac{7}{2}^-$ | ... | |
| 8.10 | 17.49 | (2)? | $(\frac{3}{2}^+)$? | ... | |
| 8.69 | 18.08 | (0)? | $(\frac{1}{2}^+)$? | ... | |
| | | $Ti^{50}(p,d)Ti^{49}$ | | | |
| 0 | 8.71 | 3 | $\frac{7}{2}^-$ | $\frac{7}{2}^-$ | 16 |
| 1.36 | 10.07 | 1 | $\surd$ | $\frac{3}{2}^-$ | 16 |
| 1.55 | 10.26 | (1) | $(\frac{1}{2}^-, \frac{3}{2}^-)$ | ... | |
| 2.23 | 10.94 | 3 | $\frac{7}{2}^-$ | $\frac{7}{2}^-$ | 16 |
| 2.45 | 11.16 | 0 | $\surd$ | $\frac{1}{2}^+$ | 16 |
| 2.62 | 11.33 | 2 | $\surd$ | $\frac{3}{2}^+$ | 16 |
| 8.65 | 17.36 | (3) | $(\frac{7}{2}^-)$ | ... | |
| | | $Cr^{52}(p,d)Cr^{51}$ | | | |
| 0 | 9.82 | 3 | $\frac{7}{2}^-$ | $\frac{7}{2}^-$ | 20 |
| 0.75 | 10.58 | ... | ... | $(\frac{3}{2}^-)$ | 19 |
| 1.90 | 11.72 | (1) | ... | $(\frac{3}{2}^-)$ | 19 |
| 2.32 | 12.14 | 3 | $\frac{7}{2}^-$ | $\frac{7}{2}^-$ | 23 |
| 2.75 | 12.57 | 0 | $\frac{1}{2}^+$ | ... | |
| 2.97 | 12.79 | 2 | $\frac{3}{2}^+$ | ... | |
| 6.58 | 16.40 | 3 | $\frac{7}{2}^-$ | $\frac{7}{2}^-$ | 3 |
| | | $Fe^{54}(p,d)Fe^{53}$ | | | |
| 0 | 11.19 | 3 | $\frac{7}{2}^-$ | $\frac{7}{2}^-$ | 23, 24 |
| 0.76 | 11.95 | 1 or 3 | ... | ... | |
| 2.02 | 13.21 | 1 or 3 | ... | ... | |
| 2.83 | 14.02 | 3 | $\frac{7}{2}^-$ | ... | |
| 2.95 | 14.14 | 0 | $\frac{1}{2}^+$ | ... | |
| 3.36 | 14.55 | 3 | $\frac{7}{2}^-$ | ... | |
| 3.56 | 14.75 | 1 or 3 | ... | ... | |
| 4.24 | 15.43 | 3 | $\frac{7}{2}^-$ | ... | |
| (7.03) | 18.22 | ? | ... | ... | |
| (7.23) | 18.42 | ? | ... | ... | |
| | | $Fe^{56}(p,d)Fe^{55}$ | | | |
| 0 | 8.97 | 1 | $\surd$ | $\frac{3}{2}^-$ | 27 |
| 0.42 | 9.39 | 1 | $\surd$ | $\frac{1}{2}^-$ | 27 |
| 0.92 | 9.89 | 3 | $\frac{5}{2}^-$ | $\frac{5}{2}^-$ | 23 |
| 1.33 | 10.30 | 3 | $(\frac{7}{2}^-)$ | $(\frac{5}{2}^-)$ | 23, 29 |
| 1.41 | 10.38 | 3 | $\frac{7}{2}^-$ | $\frac{7}{2}^-$ | 23 |
| 2.90 | 11.87 | 3 | $\frac{7}{2}^-$ | $\frac{7}{2}^-$ | 25 |
| 4.45 | 13.42 | 0 | $\frac{1}{2}^+$ | ... | |
| 4.83 | 13.80 | 2 | $\frac{3}{2}^+$ | ... | |
| 7.78 | 16.75 | 3 | $\frac{7}{2}^-$ | ... | |
| | | $Fe^{58}(p,d)Fe^{57}$ | | | |
| 0, 0.014 | 7.79 | 1 | $\surd$ | $\frac{1}{2}^-, \frac{3}{2}^-$ | 20, 34 |
| 0.14 | 7.93 | 3 | $\frac{5}{2}^-$ | $\frac{5}{2}^-$ | 20 |
| 0.37 | 8.16 | 1 | $\surd$ | $\frac{3}{2}^-$ | 34 |
| 0.71 | 8.50 | 3 | $(\frac{5}{2}^-)$ | ... | |
| 2.21 | 10.00 | 3 | $\frac{7}{2}^-$ | $\frac{7}{2}^-$ | 23 |
| 3.19 | 10.98 | 3 | $\frac{7}{2}^-$ | ... | |
| 4.97 | 12.76 | (3) | $(\frac{7}{2}^-)$ | ... | |
| 5.27 | 13.06 | 2 | $\frac{3}{2}^+$ | ... | |
| 10.45 | 18.24 | (3) | $(\frac{7}{2}^-)$ | ... | |
| | | $Ni^{58}(p,d)Ni^{57}$ | | | |
| 0 | 9.98 | 1 | $\surd$ | $\frac{3}{2}^-$ | 23 |
| 0.78 | 10.76 | 3 | $\frac{5}{2}^-$ | ... | |
| 1.12 | 11.10 | 1 | $(\frac{1}{2}^-, \frac{3}{2}^-)$ | $(\frac{1}{2}^-, \frac{3}{2}^-)$ | 23, 24 |
| 2.59 | 12.57 | 3 | $\frac{7}{2}^-$ | $(\frac{5}{2}^-, \frac{7}{2}^-)$ | 23 |
| 3.23 | 13.21 | 3 | $\frac{7}{2}^-$ | ... | |
| 4.20 | 14.18 | 3 | $(\frac{7}{2}^-)$ | ... | |
| 5.22 | 15.20 | 3 | $\frac{7}{2}^-$ | ... | |
| 5.57 | 15.55 | ... | ... | ... | |
| | | $Ni^{60}(p,d)Ni^{59}$ | | | |
| 0 | 9.17 | 1 | $\surd$ | $\frac{3}{2}^-$ | 27 |
| 0.33 | 9.50 | 3 | $\frac{5}{2}^-$ | $(\frac{5}{2}^-)$ | 23 |
| 0.48 | 9.65 | 1 | $\surd$ | $\frac{1}{2}^-$ | 27 |
| 0.88 | 10.05 | 1 | $\surd$ | $\frac{3}{2}^-$ | 27 |
| 1.29 | 10.46 | (1) | $\surd$ | $\frac{1}{2}^-$ | 27 |
| 1.96 | 11.13 | 3 | $\frac{7}{2}^-$ | $(\frac{7}{2}^-)$ | 23 |
| 2.63 | 11.80 | 3 | $\frac{7}{2}^-$ | $(\frac{7}{2}^-)$ | 23 |
| 3.04 | 12.21 | 3 | $\frac{7}{2}^-$ | $(\frac{1}{2}^-, \frac{3}{2}^-)$ | 24 |
| 4.17 | 13.34 | (3) | $(\frac{7}{2}^-)$ | ... | |
| 7.28 | 16.45 | 3 | $\frac{7}{2}^-$ | $\frac{7}{2}^-$ | 4 |
| | | $Ni^{62}(p,d)Ni^{61}$ | | | |
| 0 | 8.36 | 1 | $\surd$ | $\frac{3}{2}^-$ | 27 |
| 0.068 | 8.43 | 3 | $\frac{5}{2}^-$ | $\frac{5}{2}^-$ | 20 |
| 0.28 | 8.64 | 1 | $\surd$ | $\frac{1}{2}^-$ | 27 |
| 0.65 | 9.01 | 1 | $\surd$ | $(\frac{1}{2}^-, \frac{3}{2}^-)$ | 35 |
| 1.17* | 9.53 | 1(and 3?) | $\surd$ | $\frac{1}{2}^-$ and $\frac{3}{2}^-$ | 27 |
| 1.46 | 9.82 | 3 | $\frac{7}{2}^-$ | $(\frac{5}{2}^-, \frac{7}{2}^-)$ | 35 |
| (1.76) | (10.12) | ? | ... | $(\frac{1}{2}^-, \frac{3}{2}^-)$ | 35, 37 |
| (2.07)* | (10.43) | (3) | $(\frac{7}{2}^-)$ | ... | |
| (2.47)* | (10.83) | (3) | $(\frac{7}{2}^-)$ | ... | |
| 2.90 | 11.26 | 3 | $\frac{7}{2}^-$ | ... | |
| 3.28 | 11.64 | 3 | $\frac{7}{2}^-$ | ... | |
| 9.55 | 17.91 | 3 | $\frac{7}{2}^-$ | ... | |

by an energy pulse due to the summing, a coincidence between detectors I and II was used to reject these events. In addition, a multiplier pulse within the deuteron interval was required. Coincidence requirements were established in a Cosmic Model 801 system. Preamplifier outputs from detectors I, II, and III were amplified by Cosmic 901 amplifiers for coincidence and multiplication pulses.

A modified Dymec Model 2211B voltage-to-frequency converter was used for current integration of the Faraday cup current. The output of this unit, scaled by 100, was fed to the external clock input of the analyzer for automatic dead time compensation and data recording. Beam intensity for each run was adjusted to a value such that pile-up of pulses in the $\Delta E$ detector was negligible. The maximum current used was 0.2 $\mu$A.

The thickness of the targets used ranged from 0.6 to 2.6 mg/cm$^2$ (determined by weight and area measurements) in order to take advantage of the good energy definition of the beam and resolution capabilities of the detectors. The resolution attained was $\sim$100 keV and was limited by amplifier noise due to a large capacity load on the input of the preamplifier. (Using a different cable arrangement we have recently taken spectra with an over-all resolution of $\sim$70 keV. Measurements indicate that under ideal tuning conditions, the intrinsic cyclotron beam energy spread is 30 to 40 keV at 28 MeV energy.)

The detector aperture was $\frac{1}{8}$ in. in diameter and was 5.75 in. from the target. The over-all angular-resolution function from this geometry and the beam spot size was $\sim$2.5° full width. The resulting distortion of the angular distributions was negligible.

The energy scale for the counter telescope was established by use of well-established $Q$ values for the ground state $(p,d)$ transitions in $C^{12}$, $Ti^{48}$, $Ti^{50}$, $Cr^{52}$, $Fe^{58}$, $Ni^{60}$, and $Ni^{62}$. All points lay within 50 keV of an average straight line, indicating very little drift in gain or proton energy during the runs. The energy response was linear from 10 to 20 MeV (the region of interest) with a slope of 43.1$\pm$0.2 keV/channel. For $Ni^{58}$ and $Fe^{54}$ the published $Q$ values[14,15] are in error and in these cases our own values were used in the experimental summaries given below. Where possible, known excitation energies were used to find the calibration for individual runs for a more precise determination of the excitation energies of new levels. However, for the energies of the highly excited isobaric analog states, the over-all energy calibration had to be used, so that these values tend to be somewhat less accurate.

## III. EXPERIMENTAL RESULTS

Deuteron spectra from the various targets are shown in Figs. 1 to 9 in the form of counts per channel versus channel. The peaks are labeled with the excitation energies in the residual nucleus. Peaks which appear to be multiple or are otherwise uncertain are indicated by parentheses. At the bottom of each figure are shown the angular distributions for those peaks which appear to be single. Smooth curves are drawn through the points and the assigned $l$ value of the picked-up neutrons is indicated on the curve. At the right of most of the figures are known energy levels with horizontal lines whose lengths are proportional to spectroscopic factors from $(d,p)$ reactions or from other measurements of $(p,d)$ spectra (as noted in the captions) together with the $l$ and $J^\pi$ assignments.

Comparison of the present and previous $J^\pi$ assignments is made in Table I. Our $l$ values are also summarized in Table I; these assignments are based primarily on the empirical shapes of the angular distributions but with useful guidance of distorted-wave calculations. The detailed results for each target will now be described.

### $Ti^{48}(p,d)Ti^{47}$

The 25° spectrum is shown in Fig. 1. The energy levels at the right, with $l$ values, spectroscopic factors, and spin assignments are those given by Kashy and Conlon[16] on the basis of their $(p,d)$ investigation at 17.5 MeV. The latter experiment was carried out with about 80-keV resolution compared with our resolution of 120 keV. Therefore, their excitation energy values were used to make the level assignments to the peaks in Fig. 1 up to 3.18 MeV. The excitation energies of the higher states at 7.30, 8.10, and 8.69 MeV were determined from our energy calibration to an accuracy of 50 keV. We have accepted the spin assignments of the former experiment. Our results are in agreement with theirs for the resolved states in Fig. 1. No attempt was made to obtain angular distributions for the states at 2.15, 2.56, 2.81 MeV or of the multiple peaks at 3.84 and 4.30 MeV.

Kashy and Conlon assigned no $l$ values to the 3.18-MeV level, it being only weakly excited at 17.5 MeV due to the strong dependence of cross section on $Q$ value at this proton energy. However, at 28-MeV, a very good $l=3$ angular distribution is seen for this level in Fig. 1.

The state at 7.30 MeV is assumed to be the analog of the ground state ($\frac{7}{2}^-$) of $Sc^{47}$. The states at 8.10 and 8.69 MeV are probably the analogs of the states in $Sc^{47}$ at 0.80 and 1.44 MeV found in the $Ti^{48}(d,He^3)Sc^{47}$ reaction[17] and ascribed to pickup of a $d_{3/2}$ and an $s_{1/2}$ proton, respectively.

### $Ti^{50}(p,d)Ti^{49}$

The 35° deuteron spectrum is shown in Fig. 2. The energies, $S$, $l$, and $J^\pi$ values of Kashy and Conlon[16] are also displayed. Our energy values agreed with theirs within 20 keV; however, theirs are probably more accurate and have been adopted by us for the states up to 2.62 MeV. The only other distinct peak which can be

[14] *Nuclear Data Tables*, Nuclear Data Project, edited by K. Way (Printing and Publishing Office, National Academy of Science–National Research Council, Washington, D. C., 1961), Part I.

[15] V. J. Ashby and H. C. Catron, UCRL-5419.

[16] E. Kashy and T. W. Conlon, Phys. Rev. 135, B389 (1964).

[17] J. L. Yntema and G. R. Satchler, Phys. Rev. 134, B976 (1964).

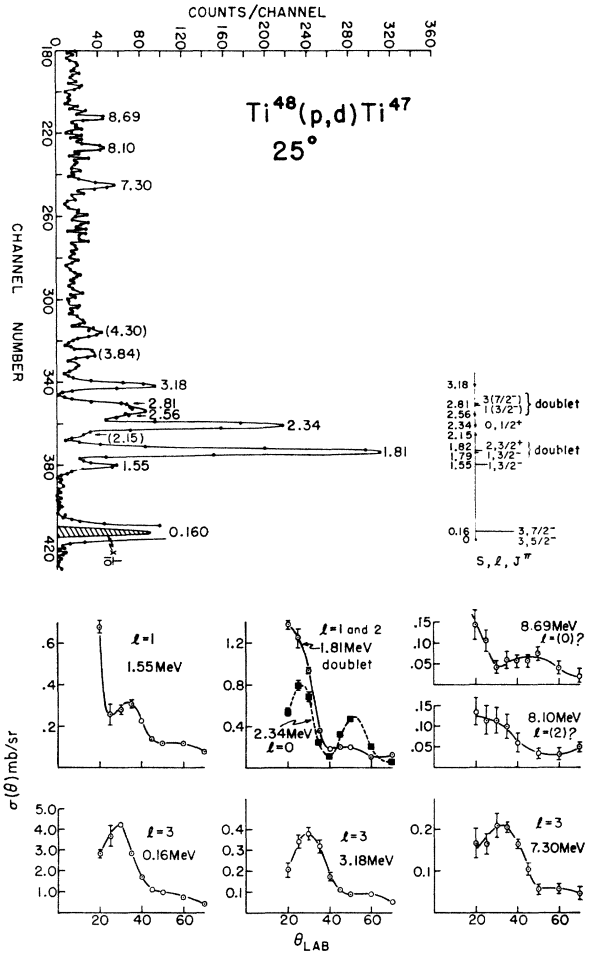


FIG. 1. The spectrum of deuterons observed at 25° from the $Ti^{48}(p,d)Ti^{47}$ reaction. The known energy levels are shown at the right. The $l$ values, spectroscopic factors and spin assignments are those of Kashy and Conlon (Ref. 16). At the bottom are shown the presently observed angular distributions for those peaks in the spectrum which appear to be single. Curves drawn through the data points have no theoretical basis.

ascribed to $Ti^{50}$ is the one labeled 8.65. This level of $Ti^{49}$ is the analog of the ground state of $Sc^{49}$.

The $Ti^{50}$ target contained 22.8% $Ti^{48}$ and 69.7% $Ti^{50}$ (plus a few percent each of $Ti^{46}$, $Ti^{47}$, and $Ti^{49}$). The peaks from $Ti^{48}$ are so labeled on the spectrum. In addition to these, the peaks corresponding to the $Ti^{49}$ levels at 2.23 and 2.45 MeV contain counts due to the 1.55 and 1.81 MeV levels of $Ti^{47}$. Correction for the latter has been made in the angular distributions shown in Fig. 2. Because of uncertainty in this correction and because the 2.23-, 2.45-, and 2.62-MeV states are not well resolved, the results for these three states must be considered as only qualitatively correct.

We might have expected to see the state in $Ti^{49}$ which is the analog of the $Sc^{49}$ state at 2.4 MeV seen by Yntema and Satchler[17] and considered by them to be due to pickup of a $d_{3/2}$ proton in the $Ti^{50}(d,He^3)$ $Sc^{49}$ reaction. The analog state would occur at an excitation of 11.1 MeV in $Ti^{49}$. No distinct peak was seen between 8.65 MeV and 13 MeV; however, with the poor statistics and large background in this energy range, the expected peak could easily be lost in the grass.

### $Cr^{52}(p,d)Cr^{51}$

The 35° spectrum for natural Cr is shown in Fig. 3. In addition to peaks from $Cr^{52}$, peaks due to $Cr^{53}$ and $Cr^{54}$ are seen at higher deuteron energy. Levels shown to the right are those found by Bochin *et al.*[18] in the $Cr^{50}(d,p)Cr^{51}$ reaction; the spin assignments are taken

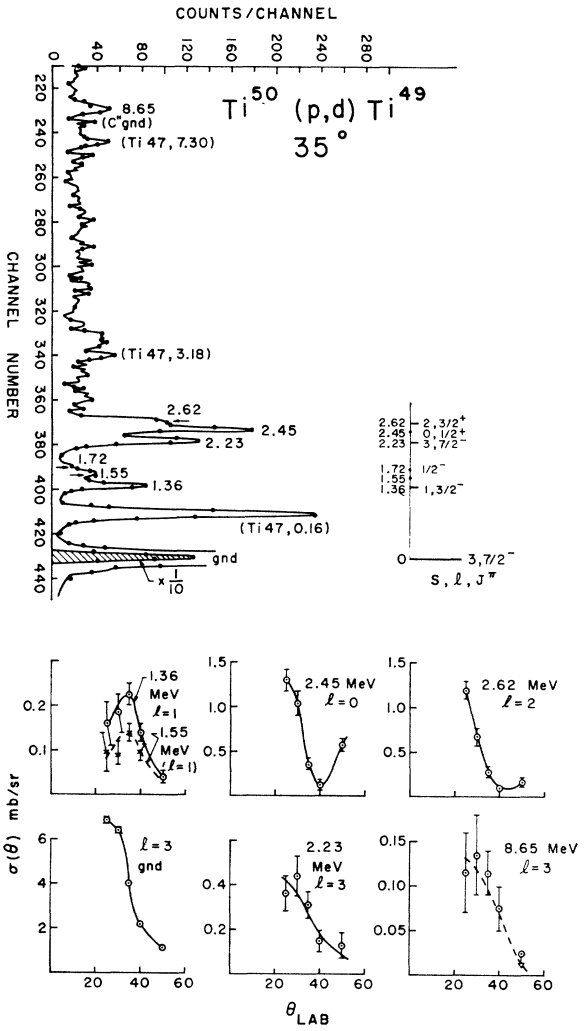


FIG. 2. The 35° spectrum of deuterons from a $Ti^{50}$ target. $S$, $l$, $J^\pi$ and the energy levels at the right are those obtained from the $(p,d)$ experiment of Kashy and Conlon (Ref. 16). Presently observed angular distributions are shown at the bottom.

[18] V. P. Bochin, K. I. Zherebtsova, V. S. Zolotarev, V. A. Komarov, L. V. Krasnov, V. F. Litvin, Yu. A. Nemilov, B. G. Novatsky, and Sh. Piskorzh, Nucl. Phys. **51**, 161 (1964).

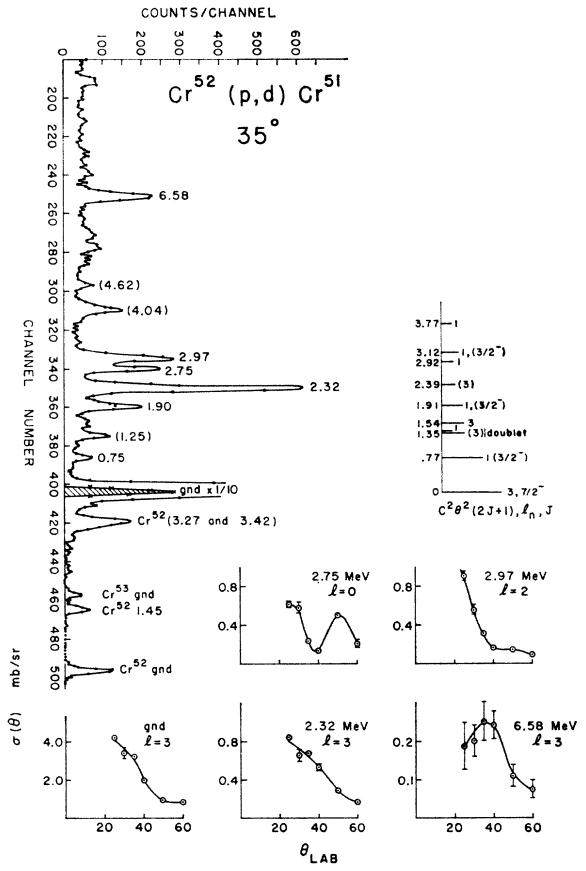


FIG. 3. The 35° spectrum of deuterons from a target of natural Cr. Known levels at the right are those reported by Bochin *et al.* (Ref. 18) from $Cr^{50}(d,p)$ measurements; the spin assignments are those of Kane *et al.* (Ref. 19). Presently observed angular distributions are shown at the bottom.

from Kane *et al.*[19] The level energies assigned to the peaks are based on our energy calibration, which is believed to be accurate to 20 keV at low energy and to 50 keV for the analog state at 6.58 MeV.

The runs on the Cr target were not entirely satisfactory. Two runs at 30° gave cross sections differing by 20%. In addition, there was a large background between the 2.32 MeV and the ground-state peaks. The angular distributions for the 0.75-, 1.25-, and 1.90-MeV states could not be assigned an unambiguous $l$ value, possibly as a result of these difficulties. The 1.90-MeV peak is probably multiple with a dominant $l=1$ component. The 1.25-MeV state has previously not been reported, a result not necessarily surprising in view of the small cross section for exciting hole states in reactions which are not of the pickup type. However, there is a peak missing from the spectrum of Fig. 3, namely the ground-state transition for the $Cr^{50}$ component of the target. Since natural chromium contains 4.4% $Cr^{50}$ and 83.7% $Cr^{52}$, and the respective $Q$ values are reported to be $-10.71$ and $-9.82$ MeV, one would expect the deuterons corresponding to the ground state of $Cr^{49}$ (if it has spin and parity $\frac{7}{2}^-$) to appear at channel 382 (0.89 MeV) with a peak count of $\sim$150. No such peak is evident. However, the 1.25-MeV peak has approximately the correct intensity. If this peak is taken to be the $Cr^{50}(p,d)Cr^{49}$ transition to the lowest $\frac{7}{2}^-$ state of $Cr^{49}$, the $Q$ value is $-11.07$ MeV. If the quoted value of the $Cr^{50}(p,d)Cr^{49}$ $Q$ value for the ground state is correct, this interpretation of the 1.25-MeV peak suggests that the ground state of $Cr^{49}$ is $\frac{5}{2}^-$ and that the $\frac{7}{2}^-$ state in $Cr^{49}$ occurs at an excitation of 360 keV. This interpretation is consistent with the assignment[20,21] of $\frac{5}{2}^-$ to the ground state of $Cr^{49}$.

Pickup experiments on $Cr^{52}$ have been carried out by Zeidman, Yntema, and Raz[22] [$(d,t)$ at 21.5 MeV], and by Legg and Rost[23] [$(p,d)$ at 18.5]. Zeidman *et al.* observed a number of weakly excited states in addition to the ground state, and ascribed $l=3$ to the 0.75-MeV state as well as to the ground state in contradiction to to the results of Bochin *et al.*,[18] and Kane *et al.*[19] Legg and Rost[23] reported seeing the ground state and a weak state at 2.22 MeV, both having $l=3$. This 2.22-MeV state is undoubtedly the 2.32-MeV state in Fig. 3.

The peaks in Fig. 3 corresponding to levels at 2.75 and 2.87 MeV are assigned $l$ values of 0 and 2 and do not correspond to previously observed levels in this region. The peaks at 4.04 and 4.62 MeV appear to be multiple and have therefore not been analyzed in detail.

The analog state at 6.58 MeV has been seen in the $V^{51}(p,n)Cr^{51}$ reaction by Anderson, Wong, and McClure.[4] Their $Q$ value for the analog state corresponds to an excitation energy of 6.54±0.10 MeV. The excellent agreement of the two measurements provides strong support for the theoretical interpretation of both types of experiments.

There are several peaks in Fig. 3 which come from the $Cr^{53}(p,d)Cr^{52}$ reaction. The ground and 1.43-MeV ($2^+$) states of $Cr^{52}$ have an $l=1$ distribution with a cross section ratio of 2:1. The broad peak corresponding to an excitation of 3.3 MeV in $Cr^{52}$ has an $l=3$ distribution and appears to consist of a doublet with energies 3.27 and 3.42 MeV. It has a cross section approximately $\frac{2}{3}$ of the $Cr^{52}(p,d)Cr^{51}$ ground state. Pickup of an $f_{7/2}$ neutron from $Cr^{53}$ should lead, on the simplest shell model, to states in $Cr^{52}$ with spin and parity $2^+$, $3^+$, $4^+$, $5^+$, with a total strength approximately equal to the $Cr^{52}(p,d)Cr^{51}$ ground-state transition. Higher resolution experiments with separated targets are clearly needed to identify the $Cr^{52}$ and low-lying $Cr^{51}$ states unambiguously.

[19] W. R. Kane, N. R. Fiebiger, and J. D. Fox, Phys. Rev. **125**, 2037 (1962).

[20] *Nuclear Data Sheets*, compiled by K. Way, *et al.* (Publishing and Printing Office, National Academy of Science–National Research Council, Washington, D. C., 1962).

[21] J. N. Ginocchio and J. B. French, Phys. Letters **7**, 137 (1963).

[22] B. Zeidman, J. L. Yntema, and B. J. Raz, Phys. Rev. **120**, 1723 (1960).

[23] J. C. Legg and E. Rost, Phys. Rev. **134**, B752 (1964).

### $Fe^{54}(p,d)Fe^{53}$

The 35° spectrum of deuterons from an isotopic target of $Fe^{54}$ is shown in Fig. 4. No previous level schemes have been reported for $Fe^{53}$. Macfarlane, Raz, Yntema, and Zeidman[24] investigated the $Fe^{54}(d,t)Fe^{53}$ reaction and observed in addition to the ground state transition, a very weak transition to a state at about 600 keV which is possibly the state we see at 760 keV. Goodman, Ball, and Fulmer[25] investigated the $(p,d)$ reaction at 22.3 MeV, but discuss only the ground-state transition, although higher states are apparent in their spectrum.

The levels of $Fe^{53}$ which appear to be single are listed in Table I. The energy values are accurate to ~30 keV, (~50 keV for the 7-MeV levels). The peaks for the ground state, 2.83-, 3.36-, and 4.24-MeV levels have reasonably definite $l=3$ angular distributions. The 0.76-, 2.02-, and 3.56-MeV levels may be either $l=1$ or $l=3$; because of poor statistics and absence of a 20° spectrum, either $l$-value fits the data.

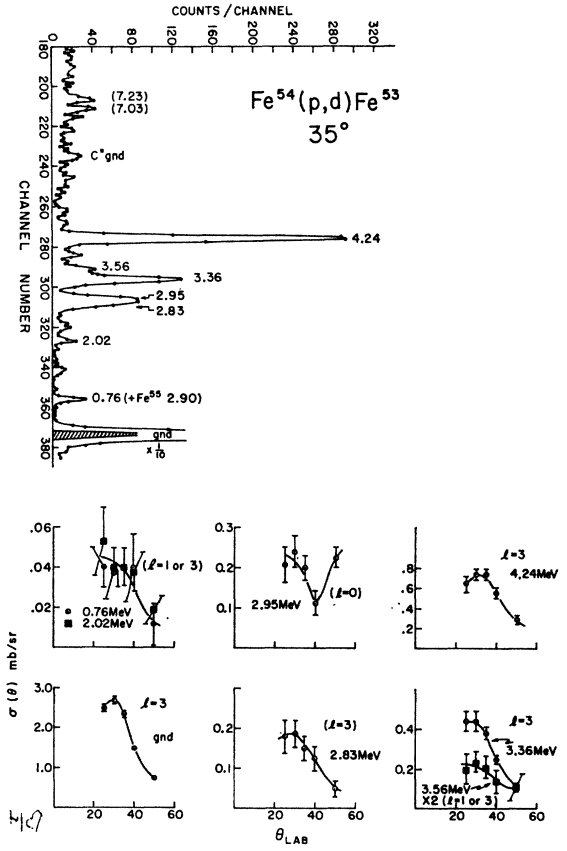


FIG. 4. The 35° spectrum of deuterons from an $Fe^{54}$ target. Observed angular distributions are shown at the bottom.

Because of the presence of 2.8% of $Fe^{56}$ in the target, the ground-state $Q$ value for the $Fe^{54}(p,d)Fe^{53}$ could be determined relative to that for $Fe^{56}(p,d)Fe^{55}$. The resulting $Q$ value is −11.19 MeV, in excellent agreement with the value of −11.20 MeV found by Legg and Rost,[23] and by Goodman *et al.*[25] but differing significantly from the published values of −11.11 MeV[15] and −11.40 MeV.[14]

Conspicuously missing from the spectrum of Fig. 4 is a peak expected near 3 MeV of excitation corresponding to the $l=2$ pickup peaks observed in $Ti^{48}$, $Ti^{50}$, $Cr^{52}$, $Fe^{56}$, and $Fe^{58}$. The expected cross section at 35° is about 200 μb/sr (interpolated from the observations on the other nuclides), corresponding to a peak half the size of the 3.36-MeV peak. An $l=2$ angular distribution should increase by a factor of four between 35° and 25°; however, none of the peaks near 3 MeV show such an increase.

### $Fe^{56}(p,d)Fe^{55}$

Figure 5 shows the 35° deuteron spectrum from an isotopic target of $Fe^{56}$, and also the angular distributions for the various peaks. The energy levels and their strengths, $(2J+1)S$, obtained from studies of the $Fe^{54}(d,p)Fe^{55}$ reaction by Fulmer and McCarthy[26] are shown on the right of the spectrum, together with the $l$ values and spins.

The spin assignments for the $\frac{1}{2}^-$ and $\frac{3}{2}^-$ states are taken from Lee and Schiffer,[27] while the $\frac{5}{2}^-$ and $\frac{7}{2}^-$ assignments are based on the relative strengths of the $l=3$ $(p,d)$ and $(d,p)$ transitions to the same state. States weakly excited in $(d,p)$ but strongly excited in $(p,d)$ are assigned spin $\frac{7}{2}^-$. Our energy values are believed to be accurate to 20 keV and agree well with previous values.

Legg and Rost[23] observed the first four peaks with the same $l$ values in the $(p,d)$ reaction at 18.5 MeV, while in a similar study at 22.3 MeV, Goodman, Ball, and Fulmer[25] observed, in addition to the first four peaks, an $l=3$ distribution for the 2.9-MeV state. [Zeidman *et al.*[22] observed the first four states in their $(d,t)$ investigation but also found states at 2.0 and 2.5 MeV which are not seen in the $(p,d)$ measurements.]

The 1.38-MeV peak was believed to be a doublet composed of the 1.327- and 1.413-MeV levels, the former contributing about 15% to the observed peak.[23] Whitten[28] in a recent $(p,d)$ measurement at 17.5 MeV was able to resolve the two states and found the ratio of the cross sections of the 1.327- and 1.413-MeV states to be 1:3.5 (similar angular distributions). Using this ratio on our $(p,d)$ data we find that the 25° cross section for the 1.327-MeV state is about twice that for the $\frac{5}{2}^-$

[24] M. H. Macfarlane, B. J. Raz, J. L. Yntema, and B. Zeidman, Phys. Rev. **127**, 204 (1962).
[25] C. D. Goodman, J. B. Ball, and C. B. Fulmer, Phys. Rev. **127**, 574 (1962).
[26] R. H. Fulmer and A. L. McCarthy, Phys. Rev. **131**, 2133 (1963).
[27] L. L. Lee, Jr., and J. P. Schiffer, Phys. Rev. Letters **12**, 108 (1964); Phys. Rev. **136**, B405 (1964).
[28] C. Whitten (private communication).

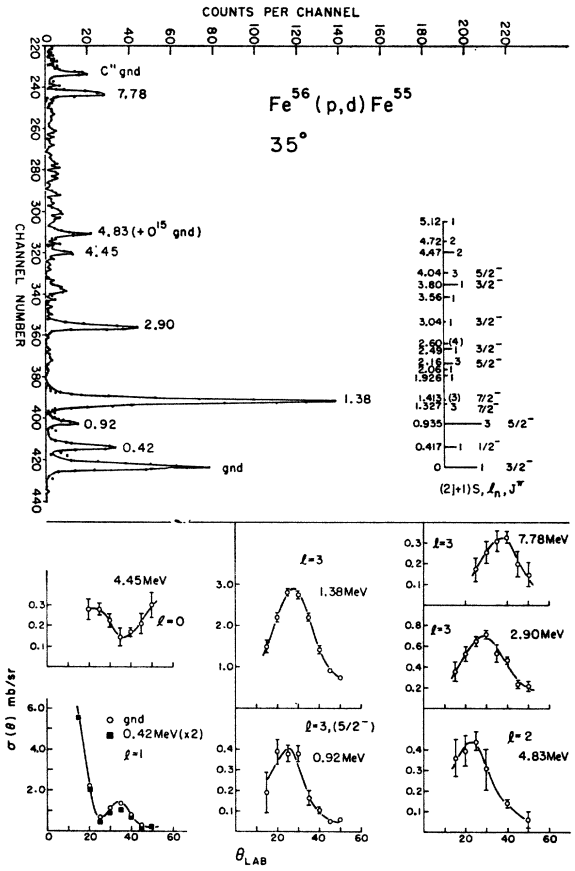


FIG. 5. The 35° spectrum of deuterons from an $Fe^{56}$ target. The energies, $l$ values, and $(2J+1)S$ are those of Fulmer and McCarthy (Ref. 26) based on $Fe^{54}(d,p)$ measurements. The spin assignments are discussed in the text. Presently observed angular distributions are shown at the bottom. The 0.92-MeV level is a $\frac{5}{2}^-$ state and is indicated in parenthesis to distinguish it from the $l=3$ angular distributions to $\frac{7}{2}^-$ states. $\frac{5}{2}^-$ states are similarly indicated in the succeeding spectra.

state at 0.92 MeV. On the other hand, the ratio of cross sections for the 1.327- and 0.92-MeV states in the $(d,p)$ experiment of Fulmer and McCarthy[26] is about one-tenth. It is therefore probable that the spin of the 1.327-MeV state is $\frac{7}{2}^-$ and it has been assigned this value in Table I. (As a consequence of this assignment, the entire cross section of the 1.38-MeV peak is used in Table V for the $\frac{7}{2}^-$ cross sections and spectroscopic factors. Should the spin of the 1.327-MeV state turn out to be $\frac{5}{2}^-$, the corresponding value of $S_{\text{exp}}$ would be reduced by about 20%.) Ramavataram[29] has assigned a spin $\frac{5}{2}^-$ to the 1.327-MeV state on the basis of a theoretical calculation. However, this question can perhaps be most satisfactorily answered by carrying out a high-resolution experiment utilizing the recently discovered $J$ dependence of the angular distributions.[27]

A forward-angle $J$ dependence of the angular distribution for $l=3$ was observed in the present investigation. This effect in $Fe^{56}$, $Fe^{58}$, $Ni^{58}$, $Ni^{60}$, and $Ni^{62}$ has been discussed in a recent publication.[30] This $J$ dependence substantiates the assignment of $\frac{7}{2}^-$ to the states showing $l=3$ angular distributions in the previously discussed targets. There is, however, one point of ambiguity in that $l=2$ angular distributions and the $l=3$ ($\frac{5}{2}^-$) distributions can be similar within the accuracy of the present measurements, as can be seen from the angular distributions for the 0.92- and 4.83-MeV states in Fig. 5. However, the latter cannot be assigned spin $\frac{5}{2}^-$, for its cross section is comparable with that of the 0.92-MeV state, yet no correspondingly strong $l=3$ transition was seen in the $(d,p)$ work.

The state in $Fe^{55}$ at 7.78±0.05 MeV is the analog of the first excited state of $Mn^{55}$ at 126 keV which has spin $\frac{7}{2}^-$. The ground state of $Mn^{55}$ has spin $\frac{5}{2}^-$. Anderson[31] and his collaborators have determined the $Q$ value for reaching the analog of the $Mn^{55}$ ground state in $Fe^{55}$ by the $(p,n)$ reaction to be $-8.53\pm0.10$ MeV. This places the $Fe^{55}$ level at $E_x=7.52\pm0.10$ MeV. The analog state we observe should, according to this result, be at $E_x=7.65\pm0.10$ MeV, in fair agreement with our observation.

### $Fe^{58}(p,d)Fe^{57}$

The deuteron spectrum at 25° is shown in Fig. 6. The energy levels $(2J+1)\theta^2$ and $l$ values observed by Sperduto *et al.*[32] in the $Fe^{56}(d,p)Fe^{57}$ reaction are shown at the right. [Similar $(d,p)$ results were reported by Cohen, Fulmer, and McCarthy.[33]] The spin assignments for $\frac{1}{2}^-$ and $\frac{3}{2}^-$ are taken from Nuclear Data Sheets[20] and from the work of Bartholomew and Gunye.[34] The 0.14-MeV level has been assigned spin $\frac{5}{2}^-$.[20]

Legg and Rost[23] attributed $l=1$ neutron pickup to the ground-state doublet (0 and 0.014 MeV) and to levels at 0.34 and 1.30 MeV. While we agree with the first two peaks, the peak near 1.30 MeV in Fig. 6 shows strong mixing of the states indicated, making any analysis questionable. They also found a strong $l=3$ peak corresponding to a level at 2.22 MeV, to which they assign spin $\frac{7}{2}^-$; our results agree with theirs. [In the earlier $(p,d)$ work of Goodman *et al.*,[25] $l=1$ pickup is attributed to multiple level peaks corresponding to 0 and 1.1 MeV and $l=3$ to a strong (multiple level) peak corresponding to 2.1 MeV. Within our considerably better resolution, the 2.21-MeV peak appears to be single.] Macfarlane *et al.*,[24] in their $(d,t)$ experiments, found $l=1$ and $l=3$ mixtures for peaks at 0 and 1.3 MeV, and $l=3$ for a peak at 2.2 MeV. In addition, they

[29] K. Ramavataram, Phys. Rev. 132, 2255 (1963).

[30] R. Sherr, E. Rost, and M. E. Rickey, Phys. Rev. Letters 12, 420 (1964).

[31] J. D. Anderson (private communication).

[32] A. Sperduto, M.I.T.-L.N.S. Progress Report, 1962, p. 67 (unpublished); F. Alba, A. Sperduto, W. W. Buechner, and H. A. Enge, Bull. Am. Phys. Soc. 7, 315 (1962).

[33] B. L. Cohen, R. H. Fulmer, and A. L. McCarthy, Phys. Rev. 126, 698 (1962).

[34] G. A. Bartholomew and M. R. Gunye, Bull. Am. Phys. Soc. 8, 367 (1963).

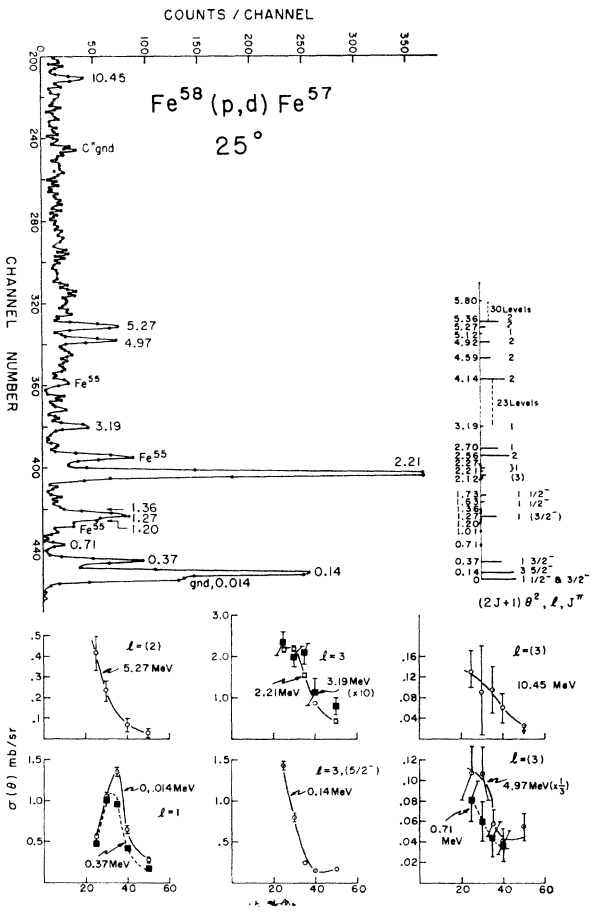


FIG. 6. The 25° spectrum of deuterons from a target of $Fe^{58}$. The energy levels, $l$ values and strengths from the $Fe^{56}(d,p)$ measurements of Sperduto *et al.* (Ref. 32) are shown. For spin-parity assignments, see text. At the bottom are the angular distributions from the present measurements.

assign $l=3(?)$ to a peak near 4.7 MeV, which may correspond to our $l=3(?)$ peak at 4.97 MeV.

The angular distributions from our measurements are shown at the bottom of Fig. 6. Note the difference in shape[30] for the $\frac{5}{2}^-$ level at 0.14 MeV and the $\frac{7}{2}^-$ level at 2.21 MeV [spins assigned on the basis of yields in the $(p,d)$ and $(d,p)$ experiments]. The angular distribution of the 5.27-MeV state is similar to that of the 0.14-MeV state; however, the former is assigned $l=2$ [cf. similar situation in $Fe^{56}(p,d)Fe^{55}$ discussed above].

Our level assignments are in general consistent with the $(d,p)$ results with regard to $l=1$ stripping levels, with, however, a conspicuous exception, namely the stripping to the 2.70-MeV level. If the latter were due to a stripping transition to a $2p$ orbital, we would expect to have seen it with a strength comparable to the 0.37-MeV peak in Fig. 6; however, the maximum yield to a level at 2.70 MeV is less than one tenth of the 0.37-MeV yield.

The 3.19-MeV level seen in the $(d,p)$ reaction has too small an $l=1$ stripping strength to be seen in the $(p,d)$ measurements. The 3.19-MeV level observed presently is assigned $\frac{7}{2}^-$ and is therefore not the 3.19-MeV level seen in stripping. The weakly excited 0.71-MeV state has an angular distribution which is consistent with either $f_{5/2}$ or $f_{7/2}$ pickup. However, it is also weakly excited (and in about the same ratio) relative to the $\frac{5}{2}^-$ 0.14-MeV state in stripping, suggesting a spin assignment of $\frac{5}{2}^-$.

### $Ni^{58}(p,d)Ni^{57}$

The deuteron spectrum at 25° is shown in Fig. 7. Previous experiments (with poorer resolution) giving information on the levels of $Ni^{57}$ have been performed using the $(d,t)$ and the $(p,d)$ reactions.[23,24] The former reported $l=1$ ground-state and 1.15-MeV transitions, and $l=1$, 3 (mixed) angular distributions to states at 0.85 and 2.5 MeV. The latter find $l=1$ transitions to the ground state and to a level at 1.04 MeV, a mixed $l=1$ and 3 transition to a state at 0.74 MeV, and an $l=3$ transition to a level at 2.46. Our data shows no evidence of appreciable $l=1$ admixtures to the 0.78 and 2.59-MeV peaks.

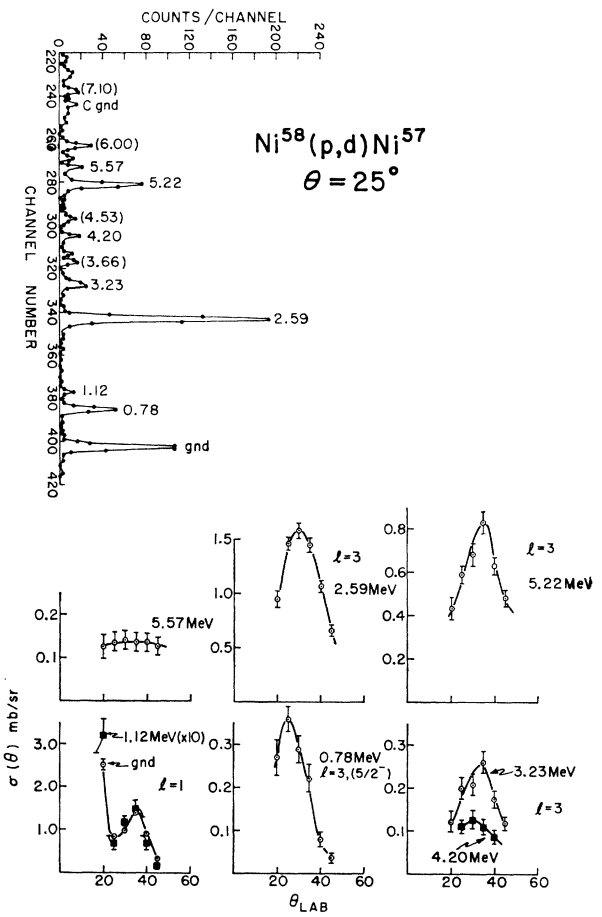


FIG. 7. The 25° spectrum of deuterons from a target of $Ni^{58}$. At the bottom are the observed angular distributions.

Although our $Q$ value for the ground-state transition is identical with that of Legg and Rost[23] ($-9.98\pm0.03$ MeV), the energies of the excited states found presently are systematically somewhat higher. Our excitation energies are believed to be accurate to $\pm20$ keV.

The state at 5.22 MeV is the analog of the ground state of $Co^{57}$. The nature of the higher excited states [5.57, (6.00) and (7.10) MeV] is not evident from our measurements. The 0.78-MeV state has been assigned a spin $\frac{5}{2}^-$ on the basis of the similarity of its angular distribution with those for $\frac{5}{2}^-$ states in $Fe^{55}$ and $Fe^{57}$ (see Ref. 30). The other $l=3$ states are assigned spin $\frac{7}{2}^-$.

### $Ni^{60}(p,d)Ni^{59}$

The 30° spectrum of deuterons from a $Ni^{60}$ target is shown in Fig. 8. A partial energy level diagram for states observed in the $(d,p)$ reaction is shown on the right, as given by Fulmer, McCarthy, Cohen, and Middleton[35] and by Moriyasu, Adams, and Enge.[36] Only those levels of interest to the present investigation are shown. The $\frac{1}{2}^-$ and $\frac{3}{2}^-$ assignments are taken from Lee and Schiffer.[27] The $\frac{5}{2}^-$ and $\frac{7}{2}^-$ assignments are based on the ratio of yields in the $(d,p)$ and $(p,d)$ experiments. The latter observations were made by Legg and Rost[23] who found states at 0, 0.34, 0.47, 0.91, 1.29, 1.90, and 2.64 MeV. Our $l$-value assignments agree with theirs. However, on the basis of the $J$ dependence of the shape of the $l=3$ distributions at 28 MeV,[30] we have made the assignments given in Table I.

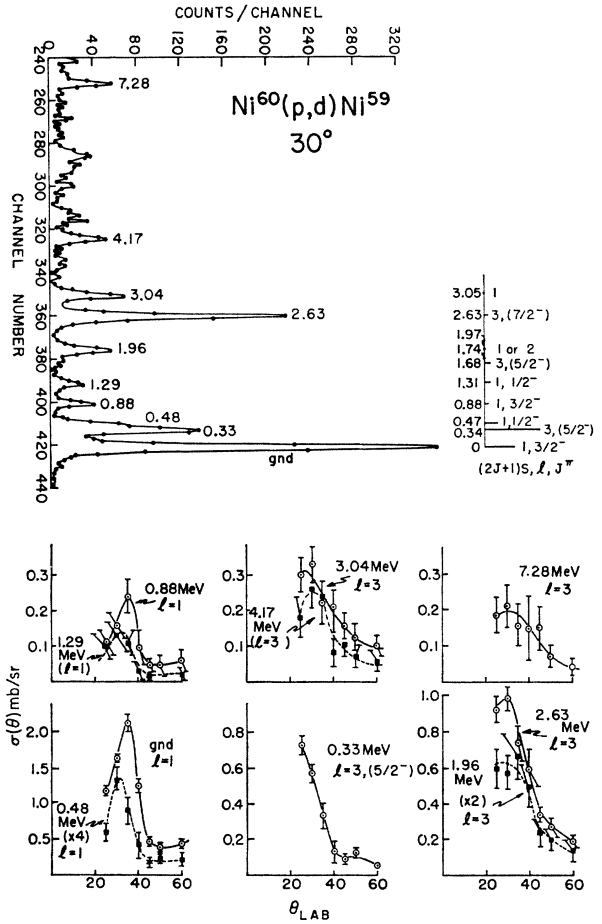


FIG. 8. The 30° spectrum of deuterons from a target of $Ni^{60}$. A partial energy level diagram is shown at the right for states observed in $Ni^{58}(d,p)$, (Refs. 35 and 36). For spin assignments, see text. Present angular distributions are shown at the bottom.

Macfarlane *et al.*[24] made essentially the same assignments of $l$ values in their $(d,t)$ work, with the exception of the state at 3.04 MeV for which they find an $l=1$ shape, whereas we find $l=3$.

Our energy values agree with those from the $(d,p)$ measurements within our estimated accuracy ($\pm20$ keV). (The energy of the isobaric analog state at 7.28 MeV is accurate to 50 keV.) For the low-lying states, the presently observed $l$ values are identical with those seen in the $(d,p)$ reaction, with the exception of the 3.04-MeV level to which we assign $l=3$ rather than $l=1$.

The isobaric analog state at $7.28\pm0.05$ keV has previously been seen by Anderson, Wong, and McClure.[4] Their $Q$ value for this state as seen in the $Co^{59}(p,n)$ reaction corresponds to an excitation energy of 7.26 $\pm0.10$ MeV. The agreement between the two determinations is excellent.

### $NI^{62}(p,d)Ni^{61}$

The 35° deuteron spectrum from $Ni^{62}$ is shown in Fig. 9. Note the absence of any definite peaks between the 3.28-MeV peak and the peak corresponding to the analog state at 9.55 MeV. The energy levels, strengths, and $l$ values from the $(d,p)$ reaction are shown to the right. This data is taken from the work of Fulmer, McCarthy, Cohen, and Middleton[35] and of Enge and Fisher.[37] (Many levels which are not immediately relevant have been omitted for clarity.) The $\frac{1}{2}^-$ and $\frac{3}{2}^-$ assignments are taken from Lee and Schiffer[27]; the $\frac{5}{2}^-$ assignment to the 0.068-MeV state is given in *Nuclear Data Sheets*[20] and is supported by the shape of the angular distribution in the present reaction.[30] We have taken the energies for the first three excited states from the $(d,p)$ results; the remaining peaks bear our energy assignments.

The angular distributions of the deuteron groups are shown in Fig. 9. The first four levels agree in $l$ assignments with those from the $(d,p)$ work. The 1.17-MeV peak has an $l=1$ distribution with possibly a small amount of $l=3$. We interpret this result to signify that the 1.17-MeV peak is mostly a mixture of the 1.11 and

[35] R. H. Fulmer, A. L. McCarthy, B. L. Cohen, and R. Middleton, Phys. Rev. **133**, B955 (1964).

[36] K. Moriyasu, J. L. Adams, and H. A. Enge, M.I.T.-L.N.S. Progress Report 1962 (unpublished).

[37] H. A. Enge and R. A. Fisher, M.I.T.-L.N.S. Progress Report 1959 (unpublished).

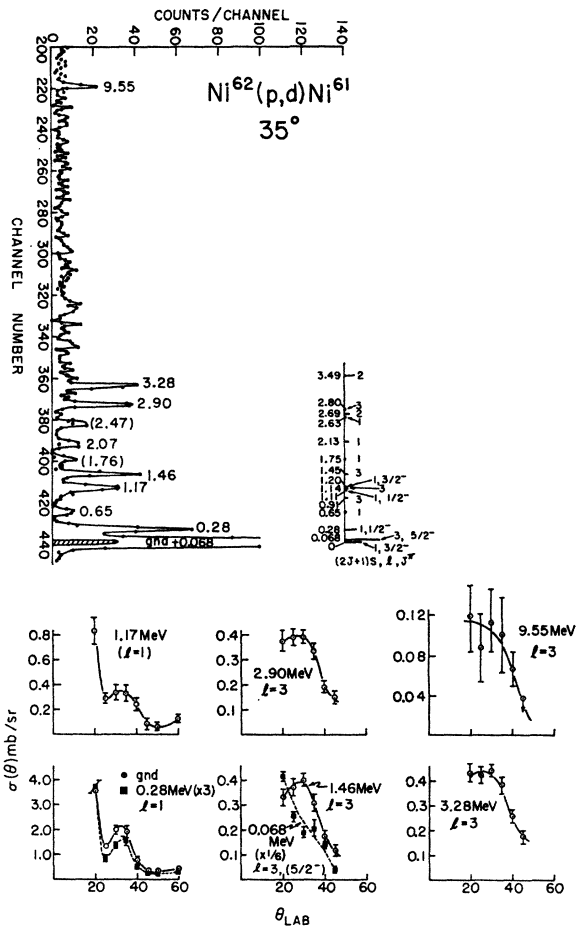


FIG. 9. The 35° spectrum of deuterons from a target of $Ni^{62}$. The energy levels, $l$ values, and strengths from $(d,p)$ measurements (Refs. 35 and 37) are shown at the right. For spin assignments, see text. The present angular distributions are shown at the bottom.

1.20-MeV levels which show $l=1$ angular distributions in the $(d,p)$ reaction. The 1.14- and 0.91-MeV levels, which exhibit $l=3$ in the $(d,p)$ reaction, are at best only weakly excited in the $(p,d)$ reaction, suggesting a spin assignment of $\frac{5}{2}^-$ to both states. The 1.46-MeV $(l=3)$ level is assigned a spin $\frac{7}{2}^-$ because of its strength in the $(p,d)$ and $(d,p)$ reactions relative to that for the lower $l=3$ and also because of its angular distribution. We have not been able to assign an $l$ value to the 1.76-MeV peak. The 2.07-MeV and the 2.47-MeV peaks are multiple; both appear to be mostly $l=3$.

## IV. DISCUSSION AND COMPARISON WITH THEORY

The detailed discussion of the experimental results will be limited to the isobaric analog states and the configuration states which are excited by $l=3$ pickup. The correctness of our assumption that the highest state having an $l=3$ angular distribution is the isobaric analog state is most convincingly established by extracting the Coulomb displacement energies from the excitation energies of these states. Section A discusses this question.

The strengths with which the various $l=3$ states are excited can be compared with detailed nuclear models after account is taken of the dependence of cross section on the various parameters contained in the dynamics of the reaction. Section B describes the analysis of the data using distorted wave (DW) calculations to extract spectroscopic factors. Comparison of the above with values predicted on the basis of shell-model sum rules shows that agreement can be obtained only by modifying the usual prescriptions of the DW method.

With the latter modification, level-by-level comparison of experiment and theory is made in Sec. C for the nuclei for which all particles in excess of 40 can be assumed to be in $1f_{7/2}$ states. Finally, in Sec. D, the observed energy splitting between the $T_0+\frac{1}{2}$ and the $T_0-\frac{1}{2}$ states is discussed with reference to theoretical predictions.

### A. Coulomb Displacement Energies

With the assumption of charge independence of nuclear forces, the mass difference $\Delta M$ between isobaric analog states is given by

$$\Delta M=\Delta E_c-(n-H),$$

where $\Delta E_c$ is the Coulomb energy difference (or Coulomb displacement energy); $\Delta M$ is given by the mass difference (mega-electron volts) between the ground states plus the excitation energy $E_x$ of the isobaric analog state. The various quantities are conveniently combined in the following form:

$$\Delta E_c=E_x+(S_n-S_p),$$

where $S_n$ and $S_p$ are the neutron and proton separation energies for the target nucleus. Our results are summarized in Table II. The analog states observed in the $(p,d)$ reaction have spin-parity $\frac{7}{2}^-$ and, therefore, the above formula is correct if the ground state of the $(Z-1)$ isobar is also $\frac{7}{2}^-$. If the $\frac{7}{2}^-$ state is an excited state, as in the case of $Mn^{55}$, $S_p$ must be correspondingly increased before computing $\Delta E_c$. In addition to $Mn^{55}$, this may also apply to $Mn^{57}$; in all other cases the ground-state spins have been determined to be $\frac{7}{2}$ or are inferred from $\beta$ decay to be $\frac{7}{2}$. The internal consistency of $\Delta E_c$ for this group of nuclei and comparison with other measurements of $\Delta E_c$ support the above interpretation of our data. For $Mn^{57}$, the large uncertainty in $(S_n-S_p)$ makes it impossible to decide whether or not its ground state spin is $\frac{7}{2}$.

Comparison of the present values of $\Delta E_c$ with previous determinations is presented in Table III. The fifth column lists the method used in each case and the corresponding references are given in the sixth column.

TABLE II. Coulomb displacement energies ($\Delta E_c$) obtained from the experimentally observed excitation energies ($E_x$) of the isobaric analog states. The sources for $S_n$ and $S_p$, the neutron and proton separation energies, are indicated in the footnotes in the table. All energies are in mega electron volts.

| Residual nucleus | $Ti^{47}$ | $Ti^{49}$ | $Cr^{51}$ | $Fe^{53}$ | $Fe^{55}$ | $Fe^{57}$ | $Ni^{57}$ | $Ni^{59}$ | $Ni^{61}$ |
|---|---|---|---|---|---|---|---|---|---|
| $E_x$ | 7.33±0.05 | 8.65±0.05 | 6.58±0.05 | 4.24±0.05 | 7.78±0.05 | 10.45±0.05 | 5.22±0.05 | 7.28±0.05 | 9.55±0.05 |
| $S_n-S_p$ | 0.18±0.01[a] | −1.20±0.02[b] | 1.54±0.01[a] | 4.56±0.05[c] | 1.01±0.01[a] | −1.92±0.20[a] | 4.02±0.02[d] | 1.86±0.01[a] | −0.50±0.04[a] |
| $\Delta E_c$ | 7.51±0.05 | 7.45±0.05 | 8.12±0.05 | 8.80±0.07 | 8.66±0.05[e] | 8.53±0.20 | 9.24±0.05 | 9.14±0.05 | 9.05±0.07 |

[a] From Refs. 14 and 15.
[b] $S_p$ obtained from $Q$ value for $Ca^{48}(He^3,d)Sc^{49}$, given by J. R. Erskine, J. P. Schiffer, and A. Marinov [Bull. Am. Phys. Soc. 9, 80 (1964)].
[c] $S_n$ obtained from $Q(p,d) = -11.19$ MeV (see Table I).
[d] $S_n-S_p$ from J. Konijn, H. L. Hagedoorn, and B. van Nooijen [Physica 24, 129 (1958)]. Using $Q(p,d) = -9.98$ (see Table I), one finds $S_n = 12.21$ MeV and $S_p = 8.19$MeV both about 270 keV higher than those of Refs. 14 and 15.
[e] $\Delta E_c$ computed with respect to $7/2^-$ state of $Mn^{55}$ at 126 keV.

The fourth column gives $\Delta E_c^r$ which is called for convenience the "reduced" Coulomb displacement energy, defined as $\Delta E_c$ for $A=2Z$, where $Z$ is the higher charge of each pair. It is obtained from the values of $\Delta E_c$ in column three by multiplying by $(A/2Z)^{1/3}$.

In view of the appreciable range of isotopes contained in Table III it is interesting to see what conclusions can be drawn regarding the charge distribution and matter distribution in this series of nuclei. If these distributions were identical and both increased radially as $A^{1/3}$, the values of $\Delta E_c^r$ would be constant for a given $Z$. Examination of the values listed in Table III shows that generally the Coulomb displacement energies do decrease with $A$ in qualitative agreement with an $A^{-1/3}$

TABLE III. Summary of Coulomb displacement energies ($\Delta E_c$) obtained from various types of measurements. Those deduced from the present experiments are indicated in column 5 by "$E_x(p,d)$." The results from $(p,n)$ observations are identified by "$Q(p,n)$," while those taken from $\beta^+$ end point measurements are indicated by "$\beta^+$." Determinations from thresholds in the $(p,n)$ reaction are listed as "$(p,n)$thr." The $Ca^{40*}$ and $Sc^{41}$ energies are based on the $\gamma$-ray energies from the $Sc^{40}$ decay and from proton capture. "$(p,p)$res" refers to the observation of analog states in elastic scattering. The 4th column gives the "reduced Coulomb energy" obtained from $\Delta E_c$ by an $A^{1/3}$ correction to $A=2Z$, where $Z$ is the higher charge of a pair of isobars. An asterisk (*) in columns 3 and 4 indicates the relative errors for a set of $(p,n)$ measurements (Ref. 38) for which the absolute uncertainty was ±0.10 MeV.

| Isobaric pair | $Z$ | $\Delta E_c$ (MeV) | $\Delta E_c^r$ (MeV) | Method | Ref. |
|---|---|---|---|---|---|
| $Cl^{33}$-$S^{33}$ | 17 | 6.31 ±0.05 | 6.25 ±0.05 | $\beta^+$ | a |
| $Cl^{34}$-$S^{34}$ | 17 | 6.264±0.005 | 6.264±0.005 | $(p,n)$thr | b |
| $Ar^{35}$-$Cl^{35}$ | 18 | 6.73 ±0.05 | 6.66 ±0.05 | $\beta^+$ | a |
| $K^{37}$-$Ar^{37}$ | 19 | 6.95 ±0.07 | 6.88 ±0.07 | $\beta^+$ | a |
| $K^{38}$-$Ar^{38}$ | 19 | 6.82 ±0.05 | 6.82 ±0.05 | $\beta^+$ | c, d |
| $K^{40}$-$Ar^{40}$ | 19 | 6.55 ±0.20 | 6.66 ±0.20 | $Q(p,n)$ | e |
| $Ca^{39}$-$K^{39}$ | 20 | 7.23 ±0.06 | 7.16 ±0.06 | $\beta^+$ | a |
| | | 7.290±0.025 | 7.22 ±0.03 | $\beta^+$ | f |
| $Ca^{40*}$-$K^{40}$ | 20 | 7.114±0.010 | 7.114±0.010 | $Sc^{40}$ $\gamma$ decay | g |
| $Sc^{41}$-$Ca^{41}$ | 21 | 7.28 ±0.02 | 7.22 ±0.02 | $(p,\gamma)$ | h |
| $Sc^{42}$-$Ca^{42}$ | 21 | 7.193±0.015 | 7.193±0.015 | $\beta^+$ | i |
| | 21 | 7.209±0.010 | 7.209±0.010 | $(He^3,p)$ | j |
| $Ti^{45}$-$Sc^{45}$ | 22 | 7.58 ±0.03* | 7.64 ±0.03* | $Q(p,n)$ | k |
| $Ti^{47}$-$Sc^{47}$ | 22 | 7.51 ±0.05 | 7.68 ±0.05 | $E_x(p,d)$ | |
| $Ti^{49}$-$Sc^{49}$ | 22 | 7.45 ±0.05 | 7.72 ±0.05 | $E_x(p,d)$ | |
| $V^{46}$-$Ti^{46}$ | 23 | 7.847±0.012 | 7.847±0.012 | $\beta^+$ | i |
| | | 7.835±0.005 | 7.835±0.005 | $(p,n)$thr | j |
| | | 7.80 ±0.04* | 7.80 ±0.04* | $Q(p,n)$ | k |
| $V^{47}$-$Ti^{47}$ | 23 | 7.81 ±0.04* | 7.87 ±0.04* | $Q(p,n)$ | k |
| $V^{48}$-$Ti^{48}$ | 23 | 7.74 ±0.03* | 7.85 ±0.03* | $Q(p,n)$ | k |
| $V^{49}$-$Ti^{49}$ | 23 | 7.73 ±0.03* | 7.89 ±0.03* | $Q(p,n)$ | k |
| $V^{50}$-$Ti^{50}$ | 23 | 7.74 ±0.03* | 7.96 ±0.03* | $Q(p,n)$ | k |
| $Cr^{51}$-$V^{51}$ | 24 | 8.12 ±0.05 | 8.29 ±0.05 | $E_x(p,d)$ | |
| | | 8.04 ±0.03* | 8.21±0.03* | $Q(p,n)$ | k |
| $Mn^{50}$-$Cr^{50}$ | 25 | 8.379±0.027 | 8.379±0.027 | $\beta^+$ | i |
| | | 8.412±0.005 | 8.412±0.005 | $(p,n)$thr | l |
| $Mn^{52}$-$Cr^{52}$ | 25 | 8.29 ±0.03* | 8.41 ±0.03* | $Q(p,n)$ | k |
| $Fe^{53}$-$Mn^{53}$ | 26 | 8.80 ±0.07 | 8.85 ±0.07 | $E_x(p,d)$ | |
| $Fe^{55}$-$Mn^{55}$ | 26 | 8.66 ±0.05 | 8.82 ±0.05 | $E_x(p,d)$ | |
| | | 8.53 ±0.03* | 8.69 ±0.03* | $Q(p,n)$ | k |
| $Fe^{57}$-$Mn^{57}$ | 26 | 8.53 ±0.20 | 8.79 ±0.20 | $E_x(p,d)$ | |
| $Co^{54}$-$Fe^{54}$ | 27 | 9.137±0.041 | 9.137±0.041 | $\beta^+$ | i |
| | | 9.033±0.005 | 9.033±0.005 | $(p,n)$thr | b |
| $Co^{56}$-$Fe^{56}$ | 27 | 8.79 ±0.05* | 8.90 ±0.05* | $Q(p,n)$ | k |
| $Co^{58}$-$Fe^{58}$ | 27 | 8.77 ±0.05* | 8.99 ±0.05* | $Q(p,n)$ | k |
| $Ni^{57}$-$Co^{57}$ | 28 | 9.24 ±0.05 | 9.30 ±0.05 | $E_x(p,d)$ | |
| $Ni^{59}$-$Co^{59}$ | 28 | 9.14 ±0.05 | 9.30 ±0.05 | $E_x(p,d)$ | |
| | | 9.10 ±0.15 | 9.26 ±0.15 | $Q(p,n)$ | e |
| $Ni^{61}$-$Co^{61}$ | 28 | 9.05 ±0.07 | 9.31 ±0.07 | $E_x(p,d)$ | |
| $Cu^{65}$-$Ni^{65}$ | 29 | 9.246±0.035 | 9.607±0.035 | $(p,p)$res | m |
| Cu-Ni | 29 | 9.45 ±0.13 | 9.50 ±0.13 | $Q(p,n)$ | e |
| $Zn^{63}$-$Cu^{63}$ | 30 | 9.55 ±0.12 | 9.70 ±0.12 | $Q(p,n)$ | n |
| $Zn^{65}$-$Cu^{65}$ | 30 | 9.42 ±0.12 | 9.66 ±0.12 | $Q(p,n)$ | n |
| Ga-Zn | 31 | 9.76 ±0.15 | 9.95 ±0.15 | $Q(p,n)$ | e |

[a] Reference 40.
[b] J. M. Freeman, J. H. Montague, G. Murray, R. E. White, and W. E. Burcham, Phys. Letters 8, 115 (1964).
[c] J. Jänecke and H. Jung, Z. Physik 165, 94 (1961).
[d] Y. Hashimoto and W. P. Alford, Phys. Rev. 116, 981 (1959).
[e] Reference 4.
[f] O. C. Kistner and B. M. Rustad, Phys. Rev. 112, 1972 (1958).
[g] Average of values obtained by W. C. Anderson, L. T. Dillman, and J. J. Kraushaar (to be published) and M. E. Rickey, E. Kashy, and D. Knudsen (unpublished).
[h] J. W. Butler, Phys. Rev. 123, 873 (1961).
[i] J. H. Miller, III, and D. C. Sutton (unpublished).
[j] D. Cline, H. E. Gove, and B. Cujec, Bull. Am. Phys. Soc. 10, 25 (1965).
[k] Reference 38.
[l] J. M. Freeman, G. Murray, and W. E. Burcham, *International Conference on Nuclear Physics*, Paris, July 1964 (to be published).
[m] L. L. Lee, Jr., A. Marinov, and J. P. Schiffer, Phys. Letters 8, 352 (1964).
[n] J. D. Anderson, C. Wong, and J. W. McClure, Phys. Rev. 126, 2170 (1962).

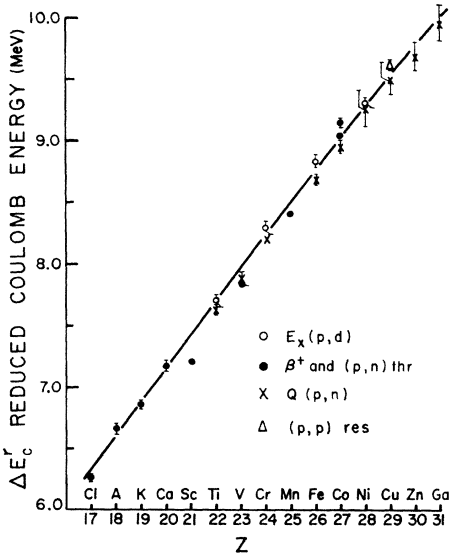


FIG. 10. Experimental values of reduced Coulomb displacement energies as a function of $Z$. The values of $\Delta E_c^r$ of Table III have been averaged for each method of determining $\Delta E_c$, as noted on the figure. $Z$ is the higher charge of a pair of isobars.

dependence, except in the V-Ti series where the $(p,n)$ measurements of Anderson *et al.*[38] indicate a significantly slower decrease with $A$ than $A^{-1/3}$.

Similar data for lighter nuclei such as $O^{14}$ and $O^{15}$, $Al^{25}$ and $Al^{26}$, etc., are consistent with an $A^{-1/3}$ dependence. Using values listed by Freeman *et al.*[39] and by Wallace and Welch,[40] the difference in $\Delta E_c$ for $O^{14}$ and $O^{15}$ is $(2.04\pm0.6)\%$; an $A^{1/3}$ correction reduces this to $(0.25\pm0.6)\%$. For $Al^{25}$ and $Al^{26}$, an $A^{1/3}$ correction reduces the difference from $(1.5\pm0.8)\%$ to $(0.1\pm0.8)\%$ while for $Cl^{34}$ and $Cl^{33}$ a similar improvement in difference is seen in Table III. (In the last two instances the errors are too large to indicate more than qualitative correctness of an $A^{1/3}$ dependence.) On the other hand, recently reported results on the isobaric analog states in $Sc^{43}$ and $Sc^{49}$ lead to values of $\Delta E_c^r$ considerably greater than those for $Sc^{41}$ and $Sc^{42}$ in Table III. The measurement[41a] for $Sc^{43}$ by Schwartz and Alford on $Sc^{43}$ yields $\Delta E_c^r = 7.30$ MeV, those of Jones *et al.*[41a] on $Sc^{49}$ give $\Delta E_c^r = 7.45$ MeV, while the corresponding values for $Sc^{41}$ and $Sc^{42}$ (Table III) are 7.22 and 7.20 MeV.

Some results relating to this question of charge and matter distribution have been obtained by electron scattering and by $\mu$-meson x-ray studies. Hahn *et al.*[41b] have investigated electron scattering from neighboring nuclei. Comparing $Ni^{58}$, $Ni^{60}$, and $Fe^{56}$ they find that the observed variation of the ratios of cross section with angle can be accounted for by an $A^{1/3}$ dependence of the charge distribution; at the least, the two extra neutrons in $Ni^{60}$ affect the proton structure of Ni. Recent measurements[41c] of $\mu$-mesonic x-rays from Mo isotopes by Chasman *et al.*[41c] yield results in fair agreement with an $A^{1/3}$ dependence although similar earlier experiments by Cohen *et al.*[41c] on Ca, Sn, and O indicate isotope shifts less than half as great. To summarize, it appears that the $A^{1/3}$ dependence seems to be valid for some nuclei and not for others.

In Fig. 10 we have plotted $\Delta E_c^r$ versus $Z$. The values of $\Delta E_c^r$ of Table III have been averaged where there is agreement between separate determinations. Because of their large uncertainties, the $K^{40}$-$Ar^{40}$ and $Fe^{57}$-$Mn^{57}$ values have been omitted. The agreement between the various sources of $\Delta E_c^r$ is in general good, with the exception of the Fe and Co values. The values for Sc are notably low with respect to the curve, showing a significant shell effect over and above the general tendency of odd-$Z$ points to lie lower than the even-$Z$ points. The latter effect was considered by Feenberg and Goertzel[42] in 1946. They ascribed the effect to the fact that proton pairs with antiparallel spins have space-symmetric wave functions in their relative coordinates and therefore repel each other more strongly than spin-symmetric pairs. Because the number of the former is $[\frac{1}{2}Z]$, the largest integer which does not exceed $\frac{1}{2}Z$, it does not increase in going from even to odd $Z$; hence, the Coulomb energy difference for odd $Z$ increases less rapidly than the values for neighboring even $Z$. The major part of the Coulomb energy comes from the remaining $\frac{1}{2}Z(Z-1)-[\frac{1}{2}Z]$ statistical pairs of protons, so that the odd $Z$-even $Z$ effect is small. The work of Feenberg and Goertzel[42] was extended by Carlson and Talmi[43] who discussed this question from the point of view of the shell model. Wallace and Welch[40] and Jänecke[44] have re-examined this odd-even effect using more recent experimental data.

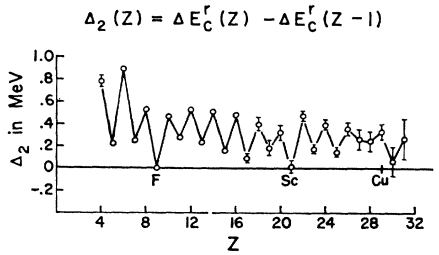


FIG. 11. Second Coulomb energy differences, $\Delta_2$, as a function of $Z$. $\Delta_2$ is defined on the figure. The values of $\Delta E_c^r$ used was averaged over the various determinations listed in Table III for $Z \geq 17$; for lower values of $Z$, the compilation of Jänecke (Ref. 44) was used.

[38] J. D. Anderson, C. Goodman, and C. Wong (unpublished).
[39] J. M. Freeman, J. H. Montague, D. West, and R. E. White, Phys. Letters **3**, 136 (1962).
[40] R. Wallace and J. A. Welch, Jr., Phys. Rev. **117**, 1297 (1960).
[41] (a) J. J. Schwartz and W. P. Alford, Bull. Am. Phys. Soc. **10**, 479 (1965); K. W. Jones, L. L. Lee, Jr., A. Marinov, and J. P. Schiffer, *ibid.* **10**, 479 (1965). (b) B. Hahn, R. Hofstadter, and D. G. Ravenhall, Phys. Rev. **105**, 1353 (1957). (c) C. Chasman, R. A. Ristinen, R. C. Cohen, S. Devons, and C. Nissim-Sabat, Phys. Rev. Letters **14**, 181 (1965); R. C. Cohen, S. Devons, A. D. Kanaris, and C. Nissim-Sabat Phys. Letters **11**, 70 (1964).
[42] E. Freenberg and G. Goertzel, Phys. Rev. **70**, 597 (1946).
[43] B. C. Carlson and I. Talmi, Phys. Rev. **96**, 436 (1954).
[44] J. Jänecke, Z. Physik **160**, 171 (1960).

The alternation of $\Delta E_c$ with $Z$ is best seen by plotting $\Delta_2(Z)=\Delta E_c{}^r(Z)-\Delta E_c{}^r(Z-1)$ versus $Z$, as is done in Fig. 11. The values for $Z\geqslant 17$ were obtained from Table III after averaging the values of $\Delta E_c{}^r$, while for lower $Z$ the compilation of Jänecke[44] was used. The values of $\Delta_2$ for F and Sc are the lowest and reflect the reduced Coulomb interaction when the last proton is in a new orbital. The alternation persists clearly up to Fe ($Z=26$), but beyond this, the effect seems to disappear or even to change phase. The washout appears just in the region where, because of the increasing neutron excess, the analog state begins to have a sizeable fraction of its wave function with a proton in the $2p$ shell.

For the nuclei from Sc through Mn in Table III, the protons in excess of 20 are presumed to be in the $1f_{7/2}$ shell.

However, if the $\frac{7}{2}^-$ state of $Mn^{55}$ is described schematically as

$$\begin{matrix} p_{3/2}: \\ f_{7/2}: \\ \quad p \end{matrix}\begin{pmatrix} & 2 \\ 5 & 8 \end{pmatrix}\begin{matrix} \\ \\ n \end{matrix},$$

the analog state in $Fe^{55}$ is

$$\sqrt{\tfrac{3}{5}}\begin{pmatrix} & 2 \\ 6 & 7 \end{pmatrix}+\sqrt{\tfrac{2}{5}}\begin{pmatrix} 1 & 1 \\ 5 & 8 \end{pmatrix}.$$

The second component, having a proton in the $p_{3/2}$ shell, will not contribute as strongly as the first component to the Coulomb energy. Such an effect would be even greater for the Ni isotopes, for the preponderant part of the wave function for these is the component of the second kind. This argument may account for the absence of a shell effect at Cu ($Z=29$). In the case of the $Ca^{40}$ analog state of $K^{40}$ a proton has been promoted from the $d_{3/2}$ to the $f_{7/2}$ orbital. Thus, $\Delta E_c{}^r$ for this case might be expected to be appreciably lower than for $Ca^{39}$-$K^{39}$, both because the Coulomb interaction of the $1f$ proton is less and because a $d_{3/2}$ Coulomb pairing energy has been lost. Although $\Delta E_c{}^r$ is indeed lower, the decrease is not as marked for $Ca^{40}$ as it is for Sc. When more information on the details of the wave functions become available it should be possible to calculate these effects. It is apparent that more precise experimental data will also be necessary for a quantitative investigation of these questions.

### B. Distorted Wave Calculations and Summed Spectroscopic Factors

The distorted-wave (DW) theory has been described in detail elsewhere.[45] For a $(p,d)$ reaction assuming a simple pick-up mechanism, one needs to specify the relative motion of the proton-target and deuteron-residual nucleus systems. These are conveniently obtained from an optical-model analysis of the appropriate elastic scattering experiments and are listed in Table IV. The proton parameters were obtained by analyzing[46] the elastic scattering of 28-MeV protons on $Ni^{58}$. These parameters were assumed to hold for the other nuclei except for the real well depth $V_p$ which was adjusted using the formula,[47]

$$V_p=V_p(0)+0.4ZA^{-1/3}+27(N-Z)/A \text{ MeV}, \quad (1)$$

where $V_p(0)$ is independent of $Z$ and $A$. This correction is small and does not affect the $(p,d)$ cross sections significantly.

TABLE IV. Optical-model parameters. The notation used is defined in Ref. 47. (Energies are given in MeV and lengths in F.)

| | $V_S$ | $r_{0S}$ | $a_S$ | $W_D$ | $r_{0I}$ | $a_I$ |
|---|---|---|---|---|---|---|
| Proton | 44.6[a] | 1.30 | 0.458 | 17.1 | 1.07 | 0.341 |
| Deuteron | [b] | 1.15 | 0.810 | [c] | 1.35 | 0.68 |

[a] Value for $Ni^{58}$. For other nuclei Eq. (1) was used to "correct" this value.
[b] $V_d=81+2.0ZA^{-1/3}-0.22\,E_d$.
[c] Extracted from Fig. 20 of Ref. 48.

The deuteron parameters were taken from a systematic study of Perey and Perey[48] using their geometry $B$ and employing average well depths (Figs. 17, 19, and 20 of Ref. 48) as a function of deuteron energy and atomic number. This choice was motivated by the desire to have the deuteron well depth resemble the sum of proton and neutron well depths. Some empirical evidence favoring this choice for analysis of some $(d,p)$ reactions also exists.[49] In a few cases the $Q$ values were sufficiently negative to require extrapolation of the deuteron parameters; however, the uncertainties involved in this procedure were always much less than other uncertainties to be discussed. The deuteron parameters we used have been shown to be unsatisfactory for Ca and the Ti isotopes.[17,49] However, calculations performed with a variety of deuteron optical parameters always gave similar results in the comparison of relative $(p,d)$ cross sections.

In order to compute the $(p,d)$ cross sections, one must also specify the overlap integral of the target and residual nucleus. The result is called the "wave function of the picked-up neutron" as is reasonable with an independent-particle model for the nuclear states. Since all targets were even-even, i.e., spin and parity $0^+$, the angular momentum and parity rules lead to a single $(lj)$ value for the picked-up neutron and consequently it is only necessary to consider the radial wave function $u_{lj}(r)$ of the picked-up neutron. It has become customary in DW calculations to specify the geometry of a central well (e.g., a well of Woods-Saxon shape with radius 1.25 $A^{1/3}$ F and diffusivity 0.65 F)

[45] See, e.g., R. H. Bassel, R. M. Drisko, and G. R. Satchler, Oak Ridge National Laboratory Report ORNL-3240 (unpublished); W. Tobocman, *Theory of Direct Nuclear Reactions* (Oxford University Press, New York, 1961). The Oak Ridge computer program, JULIE, was used.

[46] An optical model parameter-search routine written by F. G. Perey was employed. We are indebted to Dr. Perey for the use of this program.

[47] F. G. Perey, Phys. Rev. **131**, 745 (1963).

[48] C. M. Perey and F. G. Perey, Phys. Rev. **132**, 755 (1963).

[49] L. L. Lee, J. P. Schiffer, B. Zeidman, G. R. Satchler, R. M. Drisko, and R. H. Bassel, Phys. Rev. **136**, B971 (1964).

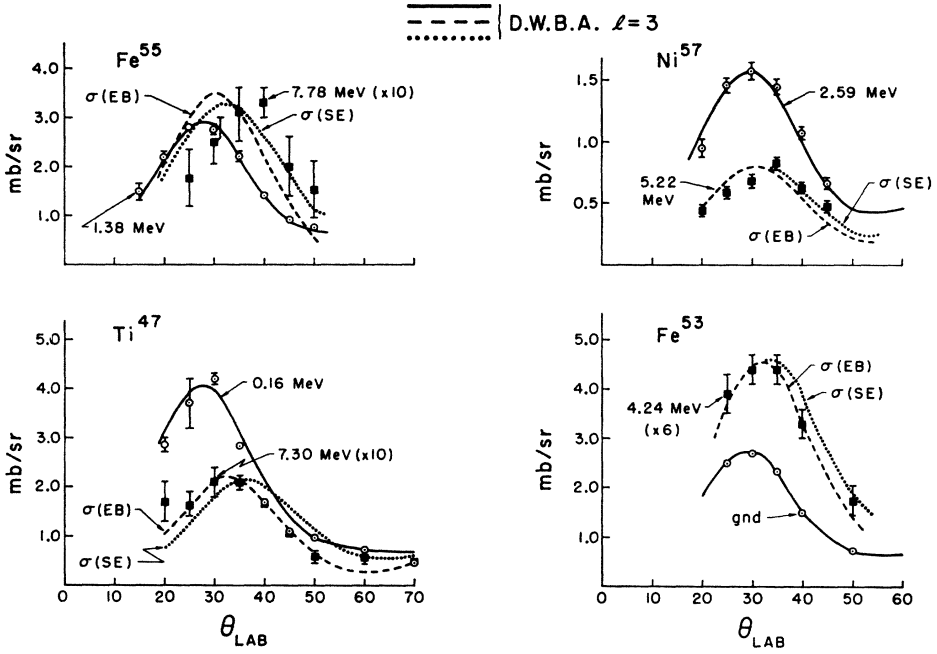


FIG. 12. Experimental and theoretical differential cross sections for $l=3$ pickup leading to the isobaric analog $\frac{7}{2}^-$ state and to the main $\frac{7}{2}^-$ configuration state in $Ti^{47}$, $Fe^{53}$, $Fe^{55}$, and $Ni^{57}$. For the analog state, two calculated curves are shown corresponding to the EB and SE descriptions of the wave function of the picked-up neutron (see text).

and then adjust the well depth to bind this neutron with the known separation energy $S=2.225-Q$. Such a procedure is certainly reasonable for closed shell targets exciting low-lying hole states [or particle states in $(d,p)$ reactions] since it is well known that such levels are well described by a hole (or particle) in a spherical well. For other nuclei this procedure is open to question, especially when the adjusted well depths are found to vary considerably for levels which are well described as being in the same configuration. Finally the $T_0+\frac{1}{2}$ analog states in $Ti^{49}$, $Fe^{57}$, and $Ni^{61}$ are unstable against $T$-forbidden neutron emission by 0.5, 2.8, and 1.7 MeV, respectively. Although these states do not show any appreciable broadening, the application of the usual DW procedure may not be valid here.

An alternative procedure is to use a fixed bound-state wave function for *all* states which arise from the same zero-order shell-model configuration. In this case the binding energy is not in general equal to the separation energy. This procedure has been called the effective binding-energy prescription[50] and may be viewed as ignoring the effect of residual interactions on the radial wave function of the picked-up neutron. Some empirical evidence has been found in a few experiments[30,51] favoring this procedure over the customary procedure using the separation energy. A recent paper[52] has discussed the problem in terms of a self-consistent potential which formally incorporates the effects of residual interactions. Unfortunately this procedure has not yet proved amenable to direct calculations. In view of the uncertainties involved in obtaining the picked-up neutron wave function and its importance in the extraction of *relative* strengths in DW calculations, we will present both the separation energy (SE) and the effective binding energy (EB) procedures. For the EB procedure we will employ wave functions which correspond to the experimental separation energy for excitation of the *lowest* $\frac{7}{2}^-$ state (This state usually contains most of the single particle $l=3$ strength.) The higher $\frac{7}{2}^-$ states will then all have the same radial wave function and will extend further radially than the SE wave functions, thus increasing the predicted $(p,d)$ cross sections. The two procedures will predict somewhat different angular distributions for the higher excited states, but as will be seen shortly, the present experimental results are not accurate enough to lead to a choice between the two on this basis.

The caliber of the agreement in shape between calculated angular distributions and the experimental data for $l=3$ pickup can be seen in Fig. 12. The data for the strongest configuration state and for the isobaric analog state is shown for $Ti^{47}$, $Fe^{53}$, $Fe^{55}$, and $Ni^{57}$. The theoretical fits for the configuration states is excellent for $Fe^{53}$, $Fe^{55}$, and $Ni^{57}$. The $Ti^{47}$ fit is less good, but this particular run showed fluctuations in yield far outside statistics in spectra taken at the same angle at different times; this lack of reproducibility is responsible for the large error flags on the 25° cross section. A more detailed comparison is shown in Fig. 13 for data on the 1.38-MeV state of $Fe^{55}$ obtained by Glashausser[53];

[50] G. R. Satchler, *Proceedings of the Conference on Nuclear Spectroscopy with Direct Reactions, Argonne, Illinois, 1964*, edited by F. E. Throw, ANL-6878 (unpublished), p. 47.
[51] J. L. Yntema, Phys. Rev. 131, 811 (1963).
[52] N. Austern, Phys. Rev. 136, B1743 (1964)

[53] C. Glashausser (private communication).

TABLE V. Summed spectroscopic factors. The symbols EB and SE refer to the effective binding and separation energy procedures used in the DW analysis. The state with highest excitation in each nucleus is the higher $T$ or analog state. An asterisk (*) refers to an unresolved doublet.

| Nucleus | $-Q$ (MeV) | $E_x$ (MeV) | $\sigma_{max}$ (mb/sr) | $\Sigma S_{exptl}$ EB | $\Sigma S_{exptl}$ SE | $\Sigma S_{exptl}/\Sigma S_{theoret}$ EB | $\Sigma S_{exptl}/\Sigma S_{theoret}$ SE |
|---|---|---|---|---|---|---|---|
| $Ti^{47}$ | 9.55 | 0.16 | 4.10±0.30 | 2.78 | 2.88 | 0.51±0.05 | 0.53±0.05 |
| | 12.57 | 3.18 | 0.38±0.03 | | | | |
| | 16.69 | 7.30 | 0.21±0.03 | 0.34 | 0.74 | 0.86±0.12 | 1.86±0.27 |
| $Ti^{49}$ | 8.71 | 0 | 7.10±0.30 | 4.10 | 4.15 | 0.53±0.03 | 0.54±0.03 |
| | 10.94 | 2.23 | 0.42±0.05 | | | | |
| | 17.36 | 8.65 | 0.13±0.03 | 0.24 | 0.68 | 0.82±0.21 | 2.34±0.47 |
| $Cr^{51}$ | 9.82 | 0 | 4.00±0.40 | 3.12 | 3.19 | 0.43±0.04 | 0.44±0.04 |
| | 12.14 | 2.32 | 0.77±0.08 | | | | |
| | 16.40 | 6.58 | 0.22±0.05 | 0.35 | 0.70 | 0.44±0.09 | 0.88±0.18 |
| $Fe^{53}$ | 11.19 | 0 | 2.60±0.20 | | | | |
| | 14.02 | 2.83 | 0.19±0.04 | 2.92 | 3.20 | 0.37±0.04 | 0.40±0.04 |
| | 14.55 | 3.36 | 0.44±0.05 | | | | |
| | 15.43 | 4.24 | 0.75±0.05 | 1.07 | 1.59 | 0.53+0.05 | 0.80±0.08 |
| $Fe^{55}$ | 10.34(*) | 1.38 | 2.90±0.20 | 2.56 | 2.65 | 0.38±0.04 | 0.39±0.04 |
| | 11.87 | 2.90 | 0.72±0.04 | | | | |
| | 16.75 | 7.78 | 0.32±0.05 | 0.64 | 1.29 | 0.54±0.08 | 1.07±0.16 |
| $Fe^{57}$ | 10.00 | 2.21 | 2.20±0.20 | | | | |
| | 10.98 | 3.19 | 0.20±0.05 | 2.03 | 2.10 | 0.28±0.03 | 0.29±0.03 |
| | (12.76) | (4.97) | 0.30±0.05 | | | | |
| | 18.24 | 10.45 | 0.12±0.05 | 0.36 | 1.00 | 0.42±0.18 | 1.16±0.48 |
| $Ni^{57}$ | 12.57 | 2.59 | 1.60±0.10 | | | | |
| | 13.21 | 3.23 | 0.25±0.03 | 2.10 | 2.12 | 0.39±0.03 | 0.40±0.03 |
| | 14.18 | 4.20 | 0.13±0.03 | | | | |
| | 15.20 | 5.22 | 0.75±0.10 | 1.17 | 1.45 | 0.44±0.06 | 0.54±0.08 |
| $Ni^{59}$ | 11.13 | 1.96 | 0.34±0.06 | | | | |
| | 11.80 | 2.63 | 1.00±0.06 | 1.84 | 2.00 | 0.29±0.02 | 0.31±0.02 |
| | 12.21 | 3.04 | 0.30±0.05 | | | | |
| | 13.34 | 4.17 | 0.24±0.05 | | | | |
| | 16.45 | 7.28 | 0.22±0.05 | 0.42 | 0.67 | 0.26±0.07 | 0.42±0.11 |
| $Ni^{61}$ | 9.82 | 1.46 | 0.37±0.05 | | | | |
| | (10.43) | (2.07) | 0.14±0.04 | | | | |
| | (10.83) | (2.47) | 0.16±0.04 | 1.13 | 1.21 | 0.18±0.02 | 0.20±0.02 |
| | 11.26 | 2.90 | 0.37±0.04 | | | | |
| | 11.64 | 3.28 | 0.42±0.04 | | | | |
| | 17.91 | 9.55 | 0.11±0.05 | 0.26 | 0.70 | 0.25±0.10 | 0.65±0.25 |

the calculated curve is identical with the one shown in Fig. 12 but is presented on a logarithmic scale. The excellent agreement is somewhat fortuitous but shows that the extraction of strength by comparing theory and experiment is unambiguous.

The data for the isobaric analog states are compared with the two prescriptions discussed above and designated as $\sigma$(EB) and $\sigma$(SE) in Fig. 12. For low excitation energy the difference in shape between the two prescriptions is too small to distinguish experimentally; this is the case for $Fe^{53}$. At higher excitation, the calculated curves are significantly different; however, the experimental peaks here are smaller and background under them higher. The appreciable disagreement between experiment and calculations for the $Fe^{55}$ 7.78-MeV state is not considered significant; considerably better measurements with three or four times greater resolution are needed in order to evaluate the significance of the apparent disagreement.

The two procedures, however, do yield quite different spectroscopic factors for highly excited states and we were in fact led to consider the EB procedure by comparison of the spectroscopic factors with sum rules based on $jj$ coupling. A very simple formula has been derived by French and Macfarlane[8] for the spectroscopic factor for exciting the $T_0+\frac{1}{2}$ state. It is

$$S_>=\pi/(N-Z+1), \qquad (2)$$

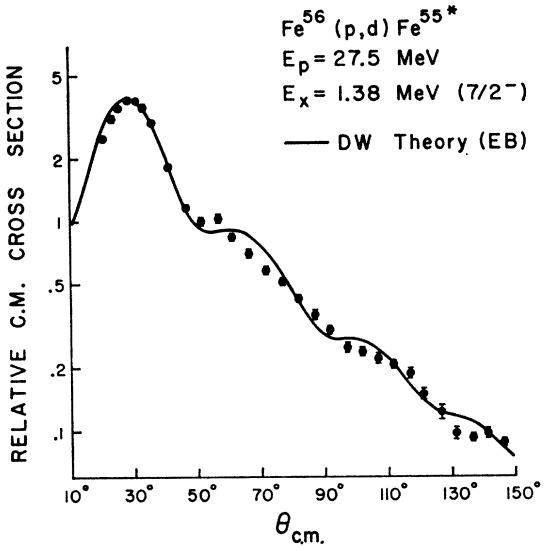


FIG. 13. Comparison of theoretical and experimental angular distributions for the 1.38-MeV ($\frac{7}{2}^-$) peak of $Fe^{55}$. The experimental data is that of Glassausser (Ref. 53).

where $\pi$ is the number of protons outside the inert core and $N$ and $Z$ are the neutron and proton numbers of the target nucleus. In principle, the left-hand side should be considered to be the sum of spectroscopic factors since there could be a spreading of the analog "state" among many 7/2 levels; in practice, however, only one such level was observed for all the nuclei studied. Since the sum of all $f_{7/2}$ neutron pickup strength is the number of such neutrons $\nu$, we can write

$$\sum S_<=\nu-\pi/(N-Z+1). \qquad (3)$$

This value is the sum of the spectroscopic factors of all $\frac{7}{2}^-$ states of lower $T$ (configuration states).

Comparison between theoretical and experimental results is made in Table V. The $\frac{7}{2}^-$ states observed in each nucleus and the corresponding $E_x$ and $\sigma_{max}(\theta)$ are listed. Individual experimental spectroscopic factors $S_{exp}$ were obtained by dividing the experimental cross section by that obtained by DW calculation. The limits of error assigned to $\sigma_{max}(\theta)$ include statistical errors, uncertainty in background corrections, and estimates of error due to differences between the observed and calculated angular distributions. The summed spectroscopic factors are given in columns 5 and 6 for the EB and SE procedures, while columns 7 and 8 give the result of dividing appropriately by the theoretical strengths, Eqs. (2) and (3). The summed spectroscopic factors are also presented in graphical form in Fig. 14. It is clear that the SE procedure yields spectroscopic factors which do not agree with Eqs. (2) and (3). However, the effective-binding method does give moderately good agreement, at least in comparing the analog $T+\frac{1}{2}$ strength with the summed configuration strength in a given nucleus. The effect of the deuteron

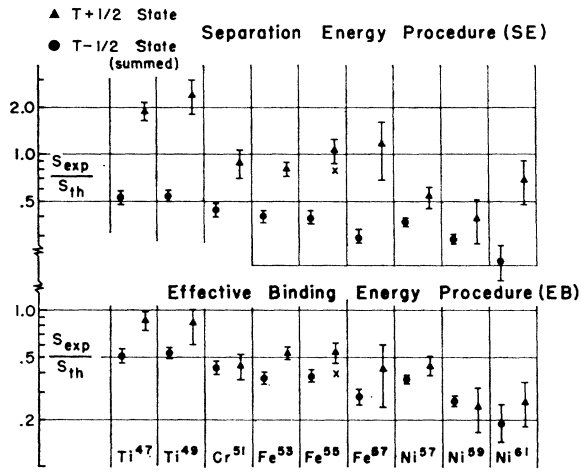


FIG. 14. Comparison of experimental and theoretical values for the summed spectroscopic factors. The upper half shows the results obtained using the SE procedure in the distorted-wave calculations, while the EB procedure leads to the values shown in the lower half of the figure. For $Fe^{55}$, the spectroscopic factor for exciting the analog state was also extracted using constant deuteron well parameters (see text) and is indicated with an $x$.

optical parameters was investigated for the $Fe^{56}(p,d)$-$Fe^{55}$ reaction. A rather extreme choice is to assume no optical-model variation with deuteron energy (or $Q$) instead of the Perey analysis where the imaginary well depth increases with decreasing deuteron energy. The result for the analog state in $Fe^{55}$ is shown by a cross in Fig. 14 and evidently does little to change the qualitative nature of the EB agreements and the SE disagreement.

An interesting trend apparent in Fig. 14 is the negative slope of $S_{\text{exp}}/S_{\text{theoret}}$ with atomic number. The absolute values do not fluctuate about unity but are rather smaller. Perhaps an extrapolation back to the $Ca^{40}$ shell closure will yield $S_{\text{exp}} \approx S_{\text{theoret}}$. It is not clear at present if this effect is due to an $A$-dependent structure effect or due to a systematic uncertainty in the DW extraction procedure. In particular the use of the lowest $\frac{7}{2}^-$ state radial wave function in the EB procedure is questionable for $Ni^{59}$ and $Ni^{61}$ where much of the $S_<$ strength comes from higher states.

The tendency for the $T-\frac{1}{2}$ points in Fig. 14 to be below the $T+\frac{1}{2}$ points may reflect the need for further refinement of the DW calculation to take account of configuration mixing. However, there may be appreciable fragmentation of the configuration levels due to $\frac{7}{2}^-$ states arising from other configurations; such fragmentation is evident in Table V for $Ni^{59}$ and $Ni^{61}$. Thus some of the $T_0-\frac{1}{2}$ strength could be spread among additional states with cross sections too small to be discerned in the present experiment, thereby reducing the observed $\sum S_<$. Such fragmentation is not expected for the analogue state since it is not observed in the corresponding $(Z-1)$ isobar. The inclusion of neglected features in the DW calculations, primarily the nonlocal effects,[54] will also increase the extracted experimental spectroscopic factors. However, they should not cause large changes in the relative comparison of states with differing $T$.

In summary, we have found that it is necessary to modify the normal procedure of distorted wave calculations to obtain agreement with the sum rules for spectroscopic factors. The discrepancy found using the SE procedure is clearly a $Q$ dependent effect as can be seen by comparing Fig. 14 with the values of $E_x$ in Table V.

### C. Individual Spectroscopic Factors and Shell-Model Calculations

In the previous section it was assumed that the $j-j$ coupling scheme was valid for the mass region under consideration. In the present section, the spectroscopic factors obtained with the EB procedure are compared with detailed predictions for those nuclei with $N$ and $Z$ not greater than 28. The theoretical calculations employ the wave functions obtained by McCullen, Bayman, and Zamick[11] for the $1f_{7/2}$ shell using the energy levels of $Ca^{42}$ and $Sc^{42}$ to determine the values for the matrix elements of the residual interaction. Although the method for extracting spectroscopic factors may be found in the literature, it is given here for the sake of completeness.

Consider the reaction $A(p,d)B$. If this is treated as a simple direct transfer, the differential cross section is usefully expressed as follows[45]:

$$\frac{d\sigma}{d\Omega}(\theta)=\sum_{nlj} S_{nlj}(J_A \rightarrow xJ_B)\sigma_{nlj}(\theta). \quad (4)$$

The spectroscopic factor $S$ is related to a generalized fractional-parentage expansion:

$$\psi_{M_A}{}^{J_A}(1\cdots Z, 1\cdots N)=\sum_{xJ_B,nlj}(xJ_B; nlj\,]\!]J_A)$$
$$\times[\psi^{xJ_B}(1\cdots Z, 1\cdots N-1)\phi^{nlj}(N)]_{M_A}{}^{J_A}. \quad (5)$$

The coefficients occurring in this expansion are generalizations of Racah's fractional parentage coefficients.[55] The index $x$ implies all the quantum numbers, in addition to $(J_B,M_B)$, needed to identify levels of the daughter nucleus; $\phi_m{}^{nlj}$ is a single-particle spin-orbit wave function, and the square bracket in (5) implies vector coupling. It is assumed in (4) that the single-particle levels $\phi_m{}^{nlj}$ and $\phi_m{}^{n\pm 1lj}$ are not simultaneously active in $\psi_{M_A}{}^{J_A}$ or $\psi_{M_B}{}^{J_B}$. The spectroscopic factor $S$ in (4) is then equal to

$$S_{nlj}(J_A \rightarrow xJ_B)=\nu(xJ_B; nlj\,]\!]J_A)^2. \quad (6)$$

where $\nu$ is the number of equivalent $(nlj)$ neutrons. It expresses the dependence of the cross section on

[54] F. G. Perey and D. S. Saxon, Phys. Letters **10**, 107 (1964).
[55] G. Racah, Phys. Rev. **63**, 367 (1943).

the detailed correlations in the target and daughter nuclei. The factors $\sigma_{nlj}(\theta)$ computed by the distorted wave method are independent of these correlations, except insofar as they affect the radial wave function of the picked-up neutron or the optical potentials of the incident or emergent particles.

According to (5), spectroscopic factors can be predicted from model wave functions. For example, suppose the ground state of $_{26}Fe_{28}^{54}$ is described as a $Ca^{40}$ core, plus six $1f_{7/2}$ protons and eight $1f_{7/2}$ neutrons. Since these neutrons form a closed shell $(1f_{7/2}^8, I_n=0)$ with angular momentum zero, the proton wave function must be the unique state $(1f_{7/2}^6, I_p=0)$. Now consider states of $_{26}Fe_{27}^{53}$ in which the nucleons in excess of $Ca^{40}$ are also confined to the $1f_{7/2}$ shell. Here the neutrons form the one-hole state $(1f_{7/2}^7, I_n=\frac{7}{2})$. The most general $_{26}Fe_{27}^{53}$ state will then be the form

$$\psi_{M_B}^{xJ_B}=\sum_{I_p} C_{I_p,7/2^{xJ_B}}[(\underset{1\cdots6}{1f_{7/2}^6}, I_p)(\underset{1\cdots7}{1f_{7/2}^7}, \tfrac{7}{2})]_{M_B}^{J_B}. \quad (7)$$

There will be four such states, corresponding to the $I_p$ values 0, 2, 4, 6. The coefficients $C_{I_p,7/2^{xJ_B}}$ may be obtained from a spectroscopic calculation, such as those of McCullen, Bayman, and Zamick[11] or Ginocchio and French.[56] We can then write the ground state of the target nucleus $Fe^{54}$ as

$$\begin{aligned}
&\psi_0^0(1\cdots6, 1\cdots8)\\
&\quad=(\underset{1\cdots6}{1f_{7/2}^6}, I_p=0)(\underset{1\cdots8}{1f_{7/2}^8}, I_n=0)\\
&\quad=(\underset{1\cdots6}{1f_{7/2}^6}, I_p=0)[(\underset{1\cdots7}{1f_{7/2}^7}, I_n=\tfrac{7}{2})\underset{8}{\phi^{1f_{7/2}}}]_0^0\\
&\quad=\{[(\underset{1\cdots6}{1f_{7/2}^6}, I_p=0)(\underset{1\cdots7}{1f_{7/2}^7}, I_n=\tfrac{7}{2})]^{7/2}\underset{8}{\phi^{1f_{7/2}}}\}_0^0\\
&\quad=\textstyle\sum_x C_{0\ 7/2^{x\ 7/2}}\{\psi^{x\ 7/2}(1\cdots6, 1\cdots7)\phi^{1f_{7/2}}(8)\}_0^0. \quad (8)
\end{aligned}$$

This expression has the form (5), and we conclude that the spectroscopic factor for the excitation of the $Fe^{53}$ state $\psi^{x\ 7/2}$ is

$$S_{1f\ 7/2}(0\rightarrow x\tfrac{7}{2})=8[C_{0\ 7/2^{x\ 7/2}}]^2. \quad (9)$$

The normalization of the state (5) implies the sum rule

$$\textstyle\sum_x S_{1f\ 7/2}(0\rightarrow x\tfrac{7}{2})=8.$$

Angular momentum and parity conservation require that pickup of $1f_{7/2}$ neutron from a $0^+$ target leads only to $\frac{7}{2}^-$ states. This requirement is, of course, exhibited by (8).

In the above model, the isobaric spin $T$ of the $Fe^{54}$ ground state is $\frac{1}{2}(8-6)=1$. States of $Fe^{53}$ can have $T=\frac{1}{2}$ or $\frac{3}{2}$, all with $T_z=\frac{1}{2}$. Each $T=\frac{3}{2}$, $T_z=\frac{1}{2}$ state will have an analog with $T=\frac{3}{2}$, $T_z=\frac{3}{2}$ in $_{25}Mn_{28}^{53}$, also within the $(1f_{7/2}^{13})$ configuration. Since there is only one such $\frac{7}{2}^-$ state, namely $(1f_{7/2}^5, I_p=\frac{7}{2})$, only one of the four states in Eq. (7) will have $T=\frac{3}{2}$, and the others (the configuration states) will have $T=\frac{1}{2}$. Since there is a unique $T=\frac{3}{2}$, $J=\frac{7}{2}^-$ state in $Fe^{53}$, the coefficient $[C_{0,\ 7/2^{T=3/2,7/2}}]^2$ is unique. It has the value 0.25, so that $S(0\rightarrow T=\frac{3}{2}, \frac{7}{2}^-)=2$. This uniquely determined $T=\frac{3}{2}$ spectroscopic factor is a special case of the French-Macfarlane sum rule, Eqs. (2) and (3). The other three coefficients of the type needed in (9) depend upon the details of the spectroscopic calculation.

[56] J. N. Ginocchio and J. B. French, Phys. Letters 7, 137 (1963).

TABLE VI. Individual spectroscopic factors for $\frac{7}{2}^-$ states compared with the McCullen-Bayman-Zamick (MBZ) theory using the effective binding (EB) procedure. An asterisk (*) denotes a rough estimate.

| Nucleus | $E_x$(exp) | $E_x$(MBZ) | $T_{MBZ}$ | $S_{MBZ}$ | $S_{exp}/S_{MBZ}$ |
|---|---|---|---|---|---|
| $Ti^{47}$ | 0.16 | 0 | $\frac{3}{2}$ | 4.77 | 0.52±0.05 |
| | 2.81 | 2.50 | $\frac{3}{2}$ | 0.14 | (∼1)* |
| | 3.18 | 2.87 | $\frac{3}{2}$ | 0.55 | 0.51±0.05 |
| | | (6 states) | $\frac{3}{2}$ | 0.14 | ··· |
| | 7.30 | 6.48 | $\frac{5}{2}$ | 0.40 | 0.86±0.12 |
| $Ti^{49}$ | 0 | 0 | $\frac{5}{2}$ | 6.68 | 0.58±0.03 |
| | 2.23 | 2.53 | $\frac{5}{2}$ | 0.59 | 0.44±0.08 |
| | ··· | 4.86 | $\frac{5}{2}$ | 0.44 | (≲0.1)* |
| | 8.65 | 8.40 | $\frac{7}{2}$ | 0.29 | 0.82±0.21 |
| $Cr^{51}$ | 0 | 0 | $\frac{3}{2}$ | 5.39 | 0.48±0.05 |
| | 2.32 | 2.62 | $\frac{3}{2}$ | 1.38 | 0.40±0.04 |
| | ··· | 5.52 | $\frac{3}{2}$ | 0.34 | (≲0.1)* |
| | 6.58 | 6.48 | $\frac{5}{2}$ | 0.80 | 0.44±0.09 |
| $Fe^{53}$ | 0 | 0 | $\frac{1}{2}$ | 4.64 | 0.47±0.04 |
| | 2.83 | | | | |
| | | 3.25 | $\frac{1}{2}$ | 1.28 | 0.58±0.06 |
| | 3.36 | | | | |
| | 4.24 | 4.17 | $\frac{3}{2}$ | 2.00 | 0.53±0.05 |
| | ··· | 5.43 | $\frac{1}{2}$ | 0.09 | ··· |

Appendix I lists $(p,d)$ spectroscopic factors calculated as in (8) for stable targets in the $1f_{7/2}$ shell, using the wave functions of McCullen, Bayman, and Zamick.[11] The calculated excitation energies of the levels are given there also. Table VI shows the comparison between theory and experiment for the targets investigated in the present experiment. With the limited resolution (∼100 keV) available to us, we have concentrated on the even-$A$ targets. Odd-$A$ spectra showed peaks at the expected positions, but the complexity of the spectra is such that measurements with better resolution are necessary for unambiguous analysis.

The calculated and observed energies in Table VI are usually in good agreement, although for $Ti^{47}$ the calculated values are consistently low. In the case of $Fe^{53}$ the 3.25-MeV level appears to be split into the observed states at 2.83 and 3.36 MeV (with a ratio of cross sections of ∼1:2). The agreement between predicted and experimental spectroscopic factors (using the EB procedure for the latter) is also reasonably good with, however, a few exceptions. The predicted levels at 4.86 MeV in $Ti^{49}$ and at 5.52 MeV in $Cr^{51}$ were not observed despite their appreciable predicted strength.

However, they lie at fairly high excitation and are fair game for fragmentation into several levels by mixing with $\frac{7}{2}^-$ states of other configurations. Indeed the 3.25-MeV level of $Fe^{53}$ appears to be split into levels at 2.83 and 3.36 MeV and assuming this, the summed strength of the latter pair is used in the table. The observed strengths of the $T_0+\frac{1}{2}$ states in $Ti^{47}$ and $Ti^{49}$ are on the high side; however, this may be due to inadequacy of the distorted wave calculation for these highly excited states.

We do not have detailed calculated wave functions for nuclei with $Z\leqslant 28$, $N>28$, so we are not in a position to use (5) and (6) to predict spectroscopic factors. However, we can postulate simple wave functions and try to use them to interpret the experimental data. For example, let us consider the two $\frac{7}{2}^-$ states in $Co^{57}$ belonging to the proton configuration $(1f_{7/2}{}^7, I_p=\frac{7}{2})$ and the neutron configuration $(1f_{7/2}{}^8, 2p_{3/2}{}^2, I_n=0, 2)$. They will be of the form

$$\begin{aligned}&\psi_m{}^{x\ 7/2}(\mathrm{Co}^{57})\\&=\sum_{L=0,2} D_L{}^{x,7/2}[(1f_{7/2}{}^7, I_p=\tfrac{7}{2})(1f_{7/2}{}^8, 2p_{3/2}{}^2; L)]_m{}^{7/2}\\&=\sum_{L=0,2} D_L{}^{x,7/2}[(1f_{7/2}{}^{15}, T=\tfrac{1}{2}, T_z=\tfrac{1}{2}, I=\tfrac{7}{2})\\&\qquad\times(2p_{3/2}{}^2, T=1, T_z=1, L)]_m{}^{7/2}. \quad (10)\end{aligned}$$

The second equation in (10) goes over to the isobaric-spin representation, as this will be more convenient for the following discussion. Actually we should also indicate antisymmetrization with respect to the different shells. We omit such indication as it has no effect on our results. The $D_L{}^{x,7/2}$ are constant coefficients whose magnitudes are determined by the effectiveness of the $(1f_{7/2}$ proton)-$(2p_{3/2}$ neutron) interaction. The extra index $x$ takes on the values 1, 2 and distinguishes the two $Co^{57}$ states that are made in this way.

The two states (10) have $T=T_z=\frac{3}{2}$, but if we act on them with the $T_-$ operator, we will get their $Ni^{57}$ isobaric analogs with $T=\frac{3}{2}$, $T_z=\frac{1}{2}$:

$$\begin{aligned}&T_-(1f_{7/2}{}^{15}, T=\tfrac{1}{2}, T_z=\tfrac{1}{2}, I=\tfrac{7}{2})\\&\quad=(\sqrt{1})(1f_{7/2}{}^{15}, T=\tfrac{1}{2}, T_z=-\tfrac{1}{2}, I=\tfrac{7}{2}),\end{aligned}$$

$$\begin{aligned}&T_-(2p_{3/2}{}^2, T=1, T_z=1, L)\\&\quad=\sqrt{2}(2p_{3/2}{}^2, T=1, T_z=0, L),\end{aligned}$$

$$\begin{aligned}&\psi_m{}^{x,7/2}(\mathrm{Ni}^{57})\\&\quad=(\sqrt{\tfrac{1}{3}})T_-\psi_m{}^{x,7/2}(\mathrm{Co}^{57})\\&\quad=\sum_{L=0,2} D_L{}^{x,7/2}\{(\sqrt{\tfrac{1}{3}})[(1f_{7/2}{}^{15}, T=\tfrac{1}{2}, T_z=-\tfrac{1}{2}, I=\tfrac{7}{2})\\&\qquad\times(2p_{3/2}{}^2, T=1, T_z=1, L)]_m{}^{7/2}\\&\qquad+(\sqrt{\tfrac{2}{3}})[(1f_{7/2}{}^{15}, T=\tfrac{1}{2}, T_z=\tfrac{1}{2}, I=\tfrac{7}{2})\\&\qquad\qquad\times(2p_{3/2}{}^2, T=1, T_z=0, L]_m{}^{7/2}\}. \quad (11)\end{aligned}$$

The $Ni^{57}$ coefficients $D_L{}^{x,7/2}$ in (11) are the same as those in the $Co^{57}$ expansion (10). In addition, $Ni^{57}$ will have four other $\frac{7}{2}^-$ states with $T=\frac{1}{2}$, all belonging to the same $(1f_{7/2}{}^{15}, 2p_{3/2}{}^2)$ configuration:

$$\begin{aligned}&\psi_m{}^{y\ 7/2}\\&\quad=\sum_{L=0,2} E_L{}^{y\ 7/2}\{\sqrt{\tfrac{2}{3}}[(1f_{7/2}{}^{15}, T=\tfrac{1}{2}, T_z=-\tfrac{1}{2}, I=\tfrac{7}{2})\\&\qquad\times(2p_{3/2}{}^2, T=1, T_z=1, L)]_m{}^{7/2}\\&\qquad-\sqrt{\tfrac{1}{3}}[(1f_{7/2}{}^{15}, T=\tfrac{1}{2}, T_z=\tfrac{1}{2}, I=\tfrac{7}{2})\\&\qquad\times(2p_{3/2}{}^2, T=1, T_z=0, L]_m{}^{7/2}\}\\&\qquad+\sum_{L=1,3} F_L{}^{y\ 7/2}[(1f_{7/2}{}^{15}, T=\tfrac{1}{2}, T_z=\tfrac{1}{2}, I=\tfrac{7}{2})\\&\qquad\qquad\times(2p_{3/2}{}^2, T=0, T_z=0, L]_m{}^{7/2}. \quad (12)\end{aligned}$$

Here the index $y$ takes on values 1 to 4.

To calculate $Ni^{58}(p,d)Ni^{57}$ spectroscopic factors we also need the $Ni^{58}$ ground-state wave function. If we take this to be $(1f_{7/2}{}^{16}, T=0, I=0)(2p_{3/2}{}^2, T=1, T_z=1, I=0)$, the $l=3$ spectroscopic factors will be $(8/3)(D_0{}^{x,7/2})^2$ for the two $Ni^{57}$ $T=\frac{3}{2}$ states, and $(16/3)(E_0{}^{y,7/2})^2$ for the four $Ni^{57}$ $T=\frac{1}{2}$ states. These are again consistent with the French-Macfarlane sum rules, Eqs. (2) and (3). If only one $T=\frac{3}{2}$ state is seen, this implies that $(D_0{}^{1,7/2})^2\gg(D_0{}^{2,7/2})^2$, indicating at the same time that the $Co^{57}$ ground state has a small $(2p_{3/2}{}^2, L_n=2)$ admixture. The experimental results show in fact only one $T=\frac{3}{2}$ state. The number of $T=\frac{1}{2}$ states to be expected is thus reduced from four to three. Experimentally, three $T=\frac{1}{2}$ states were found (see Table V). Similar analysis can be applied to $Fe^{55}$ and $Fe^{57}$; here, too, one $T_0+\frac{1}{2}$ and three $T_0-\frac{1}{2}$ states are seen in each case. For $Ni^{59}$ and $Ni^{61}$, four and five $T_0-\frac{1}{2}$ states were observed, while the $T_0+\frac{1}{2}$, states remain single. By allowing admixtures of $p_{3/2}$, $p_{1/2}$, and $f_{5/2}$ for neutrons in excess of 28, these additional $T_0-\frac{1}{2}$ states can be accounted for. Thus, the $j-j$ coupling model provides a good first approximation for interpreting the experimental results. High-resolution experiments will determine the existence of the weaker states one must expect from the observed mixing in the neutron configurations.

### D. Energy Splitting Between the $T_>$ and $T_<$ Groups

To discuss energy splitting it is necessary to assign a mean energy to the $\frac{7}{2}^-$ states of each group arising from pickup of an $f_{7/2}$ neutron. The most useful choice is

$$\begin{aligned}E_<&=\textstyle\sum_i{}^< S_iE_i/\sum_i{}^< S_i,\\E_>&=\textstyle\sum_i{}^> S_iE_i/\sum_i{}^> S_i. \quad (13)\end{aligned}$$

The $\sum_i{}^<$ sum includes the states of the $T_<$ group, $S_i$ and $E_i$ being the spectroscopic factor and energy of the $i$th such state. The mean energies, $E_<$ and $E_>$ of (13) can be reliably estimated from the data, since the states most strongly excited in the $p$-$d$ reaction make the most important contributions to the sums. The experimental results for the various targets given in Table V were used to evaluate $E_<$ and $E_>$. The latter are presented in Table VII. The EB procedure was used to obtain $S_i$ for the $T_<$ group but this choice is not at all critical here. As only one $T_>$ state was observed in all cases, $E_>$ is simply the energy of the isobaric state.

Consider first the Ni targets. Each target wave function may be regarded as a series of filled shells, up to and including $1f_{7/2}$, plus an $(A-56\equiv n)$-neutron state $\psi([p_{3/2}f_{5/2}\cdots]^n I_1=0, T_1=T_{z_1}=n/2)$. The pickup of an $f_{7/2}$ neutron adds an $f_{7/2}$-neutron hole to $\psi$. To calculate spectroscopic factors, we wish to expand this product in terms of the real states of the daughter nucleus. We do this in two stages. First, we expand the $f_{7/2}$-neutron-hole-plus-$\psi$ state in terms of isospin eigenstates,

$$(f_{7/2}^{-1},\ t=\tfrac{1}{2},\ t_z=-\tfrac{1}{2})\psi([p_{3/2}f_{5/2}\cdots]^n\ I_1=0,\ T_1=T_{z_1}=n/2)$$
$$=-\left(\frac{2T_1}{2T_1+1}\right)^{1/2}\left[(f_{7/2}^{-1},\ t=\tfrac{1}{2})\psi\left([p_{3/2}f_{5/2}\cdots]^n\ I_1=0,\ T_1=\frac{n}{2}\right)\right]_{T_1-\frac{1}{2}}^{T_1-\frac{1}{2}}$$
$$+\left(\frac{1}{2T_1+1}\right)^{1/2}\left[(f_{7/2}^{-1},\ t=\tfrac{1}{2})\psi\left([p_{3/2}f_{5/2}\cdots]^n\ I_1=0,\ T_1=\frac{n}{2}\right)\right]_{T_1-\frac{1}{2}}^{T_1+\frac{1}{2}}, \quad (14)$$

where the numerical coefficients are just the Wigner coefficients $(\frac{1}{2}T_1-\frac{1}{2}T_1|\,T_1\mp\frac{1}{2}T_1-\frac{1}{2})$. Now we expand each of the isospin eigenstates in (14) in terms of the daughter states with the corresponding isospin,

$$[(f_{7/2}^{-1},t=-\tfrac{1}{2})\psi([p_{3/2}f_{5/2}\cdots]^n\ I_1=0,T_1=n/2)]_{T_1-\frac{1}{2}}^{T_1\mp\frac{1}{2}}$$
$$=\sum_i C_i^{T_1\mp\frac{1}{2}}\psi(i,\ I=\tfrac{7}{2},\ T=T_1\mp\tfrac{1}{2},\ T_z=T_1-\tfrac{1}{2}). \quad (15)$$

The extra index $i$ distinguishes the different daughter states with the same $I$ and $T$. The coefficients in (15) obey the normalization condition

$$\sum_i (C_i^{T_1\mp\frac{1}{2}})^2=1. \quad (16)$$

According to Sec. IVC, it then follows that

$$\begin{aligned} S_i&=8(2T_1/(2T_1+1))(C_i^{T_1-\frac{1}{2}})^2, && (T_<\text{ group}),\\ S_i&=8(2T_1+1)^{-1}(C_i^{T_1+\frac{1}{2}})^2, && (T_>\text{ group}). \end{aligned} \quad (17)$$

Now consider the expectation value of the energy operator in each of the two states represented in (15):

$$\langle[(f_{7/2}^{-1},\ t=\tfrac{1}{2})\psi([p_{3/2}f_{5/2}\cdots]^n\ I_1=0,\ T_1=n/2)]_{T_1-\frac{1}{2}}^{T_1-\frac{1}{2}}|H|[(f_{7/2}^{-1},\ t=\tfrac{1}{2})\psi([p_{3/2}f_{5/2}\cdots]^n\ I_1=0,\ T_1=n/2)]_{T_1-\frac{1}{2}}^{T_1-\frac{1}{2}}\rangle$$
$$=\sum_i{}_<(C_i^{T_1-\frac{1}{2}})^2E_i,$$
$$=\sum_i{}_<S_iE_i/\sum_i{}_<S_i=E_<, \quad (18a)$$

$$\langle[(f_{7/2}^{-1},\ t=\tfrac{1}{2})\psi([p_{3/2}f_{5/2}\cdots]^n\ I_1=0,\ T_1=n/2)]_{T_1-\frac{1}{2}}^{T_1+\frac{1}{2}}|H|[(f_{7/2}^{-1},\ t=\tfrac{1}{2})\psi([p_{3/2}f_{5/2}\cdots]^2\ I_1=0,\ T_1=n/2)]_{T_1-\frac{1}{2}}^{T_1+\frac{1}{2}}\rangle,$$
$$=\sum_i{}_>(C_i^{T_1+\frac{1}{2}})^2E_i,$$
$$=\sum_i{}_>S_iE_i/\sum_i{}_>S_i=E_>. \quad (18b)$$

Subtracting (18a) from (18b), we have

$$\delta E\equiv E_>-E_<=\langle[\ ]_{T_1-\frac{1}{2}}^{T_1+\frac{1}{2}}|H|[\ ]_{T_1-\frac{1}{2}}^{T_1+\frac{1}{2}}\rangle,$$
$$-\langle[\ ]_{T_1-\frac{1}{2}}^{T_1-\frac{1}{2}}|H|[\ ]_{T_1-\frac{1}{2}}^{T_1-\frac{1}{2}}\rangle. \quad (19)$$

The only part of $H$ that can contribute to the difference on the right-hand side of (19) is that referring to the interaction between the $f_{7/2}$ hole and the target state $\psi$. Let us follow Lane[57] by representing the relevant part of the interaction by the operator

$$\beta\mathbf{t}\cdot\mathbf{T}_1=(V_1/A)\mathbf{t}\cdot\mathbf{T}_1. \quad (20)$$

Here $V_1$ is supposed to be roughly the same for all nuclei. Then (19) becomes simply

$$\delta E=\tfrac{1}{2}\beta(2T_1+1)=(V_1/2A)(N-Z+2). \quad (21)$$

The last three columns of Table VII give the values $\delta E$, $\beta$, and $V_1$, obtained from our experimental results. The three Ni cases exhibit a spread of about 30% in $\beta$ and $V_1$. However, the strength of the $T_<$ group in $Ni^{61}$ is spread over many levels and in such circumstances, it is possible that some of the higher energy $T_<$ strength has been missed and that consequently $E_<$ is really greater than the value given in Table VII. Such a correction applied to $Ni^{61}$, and to a lesser extent to $Ni^{59}$, would bring them in line with $Ni^{57}$.

French and Macfarlane[58] have discussed "$T$ splitting" in terms of the formulas (20) and (21). For the case they treated in most detail, $p_{1/2}$-neutron pickup from $Zr^{90}$,

TABLE VII. Values of $T$ splitting for observed $\frac{7}{2}^-$ states in the nuclei listed in column 1. The second column gives the neutron excess. The next two columns give the mean energy of the higher $T$ and lower $T$ states, $\delta E$ is the splitting, while $\beta$ and $V_1$ are the parameters of a $\mathbf{t}\cdot\mathbf{T}_1$ interaction which could account for the observed splitting (see text). All energies are in MeV.

| Nucleus | $N-Z$ | $E_>$ | $E_<$ | $\delta E$ | $\beta$ | $V_1$ |
|---|---|---|---|---|---|---|
| $Ti^{47}$ | 3 | 7.30 | 0.41 | 6.89 | 2.75 | 130 |
| $Ti^{49}$ | 5 | 8.65 | 0.14 | 8.51 | 2.44 | 120 |
| $Cr^{51}$ | 3 | 6.58 | 0.41 | 6.17 | 2.48 | 126 |
| $Fe^{53}$ | 1 | 4.24 | 0.81 | 3.43 | 2.28 | 121 |
| $Fe^{55}$ | 3 | 7.78 | 1.71 | 6.07 | 2.43 | 134 |
| $Fe^{57}$ | 5 | 10.45 | 2.62 | 7.73 | 2.20 | 126 |
| $Ni^{57}$ | 1 | 5.22 | 2.78 | 2.44 | 1.62 | 92 |
| $Ni^{59}$ | 3 | 7.28 | 2.80 | 4.48 | 1.79 | 106 |
| $Ni^{61}$ | 5 | 9.55 | 2.54 | 7.01 | 2.00 | 122 |

[57] A. M. Lane, Nucl. Phys. 35, 676 (1962).

[58] J. B. French and M. H. Macfarlane, Phys. Letters 2, 255 (1962).

they could account for the $T$ splitting of the $\frac{1}{2}^-$ states in $Zr^{89}$ by using $\beta=1.3$ MeV. This implies $V_1=116$ MeV, in fair agreement with the values in Table VII.

The above derivation of Eq. (21) applies only to the Ni targets, which presumably have no $1f_{7/2}$ holes of their own. It does not apply to a target such as $Cr^{52}$, which already has four $f_{7/2}$ holes. In fact, the expression (20) is meaningless in this situation. The antisymmetry of the wave function prevents us from distinguishing the $f_{7/2}$ hole created in the reaction from those already present in the target, so that we cannot say which hole is acted upon by **t**. However, we have shown in Table VII the extent to which (21) can represent the observed $\delta E$ for *all* the targets we have studied. It is clear that it provides a good semiquantitative representation over a wide range of nuclei.

TABLE VIII. Shell-model predictions (Ref. 11) for the energies and spectroscopic factors for $(p,d)$ reactions on stable targets in the $1f_{7/2}$ shell.

| $T$ | $E$ | $I$ | $S$ | $T$ | $E$ | $I$ | $S$ |
|---|---|---|---|---|---|---|---|
| | | | Even targets | | | | |
| | $Ti^{46}(p,d)Ti^{45}$ | | | | $Ti^{50}(p,d)Ti^{49}$ | | |
| $\frac{1}{2}$ | 0.28 | $\frac{7}{2}$ | 3.10 | $\frac{5}{2}$ | 0 | $\frac{7}{2}$ | 6.68 |
| $\frac{1}{2}$ | 3.87 | $\frac{7}{2}$ | 0.17 | $\frac{5}{2}$ | 2.53 | $\frac{7}{2}$ | 0.59 |
| $\frac{3}{2}$ | 4.42 | $\frac{7}{2}$ | 0.67 | $\frac{5}{2}$ | 4.86 | $\frac{7}{2}$ | 0.44 |
| $\frac{1}{2}$ | 4.75 | $\frac{7}{2}$ | 0.05 | $\frac{7}{2}$ | 8.40 | $\frac{7}{2}$ | 0.29 |
| | $Ti^{48}(p,d)Ti^{47}$ | | | | $Cr^{52}(p,d)Cr^{51}$ | | |
| $\frac{3}{2}$ | 0 | $\frac{7}{2}$ | 4.77 | $\frac{3}{2}$ | 0 | $\frac{7}{2}$ | 5.39 |
| $\frac{3}{2}$ | 2.50 | $\frac{7}{2}$ | 0.14 | $\frac{3}{2}$ | 2.62 | $\frac{7}{2}$ | 1.38 |
| $\frac{3}{2}$ | 2.87 | $\frac{7}{2}$ | 0.55 | $\frac{3}{2}$ | 3.23 | $\frac{7}{2}$ | 0.05 |
| $\frac{3}{2}$ | 4.13 | $\frac{7}{2}$ | 0.01 | $\frac{3}{2}$ | 4.96 | $\frac{7}{2}$ | 0.02 |
| $\frac{3}{2}$ | 4.55 | $\frac{7}{2}$ | 0.05 | $\frac{3}{2}$ | 5.52 | $\frac{7}{2}$ | 0.34 |
| $\frac{3}{2}$ | 5.51 | $\frac{7}{2}$ | 0.04 | $\frac{5}{2}$ | 6.48 | $\frac{7}{2}$ | 0.80 |
| $\frac{3}{2}$ | 6.11 | $\frac{7}{2}$ | 0.02 | $\frac{3}{2}$ | 6.64 | $\frac{7}{2}$ | 0.01 |
| $\frac{3}{2}$ | 6.46 | $\frac{7}{2}$ | 0.02 | | $Fe^{54}(p,d)Fe^{53}$ | | |
| $\frac{5}{2}$ | 6.48 | $\frac{7}{2}$ | 0.40 | $\frac{1}{2}$ | 0 | $\frac{7}{2}$ | 4.64 |
| | | | | $\frac{1}{2}$ | 3.25 | $\frac{7}{2}$ | 1.28 |
| | | | | $\frac{3}{2}$ | 4.17 | $\frac{7}{2}$ | 2.00 |
| | | | | $\frac{1}{2}$ | 5.43 | $\frac{7}{2}$ | 0.09 |
| | | | Odd targets | | | | |
| | $Sc^{45}(p,d)Sc^{44}$ | | | 1 | 4.00 | 1 | 0.03 |
| 1 | 0 | 2 | 0.42 | 1 | 4.02 | 5 | 0.33 |
| 1 | 0.29 | 6 | 0.49 | 1 | 4.19 | 6 | 0.07 |
| 1 | 0.28 | 1 | 0.25 | 1 | 4.89 | 6 | 0.10 |
| 1 | 0.70 | 3 | 0.28 | 1 | 5.20 | 5 | 0.29 |
| 1 | 0.86 | 4 | 0.32 | 1 | 5.21 | 4 | 0.01 |
| 1 | 1.17 | 7 | 1.43 | 1 | 5.50 | 2 | 0.03 |
| 1 | 1.30 | 5 | 0.25 | 1 | 5.60 | 3 | 0.05 |
| 1 | 2.35 | 6 | 0.01 | 1 | 6.13 | 5 | 0.03 |
| 1 | 2.52 | 3 | 0.05 | 1 | 6.44 | 6 | 0.04 |
| 2 | 2.81 | 0 | 0.17 | 1 | 6.92 | 6 | 0.03 |
| 1 | 3.01 | 1 | 0.20 | 1 | 7.19 | 4 | 0.02 |
| 1 | 3.70 | 3 | 0.02 | 1 | 7.26 | 6 | 0.04 |
| 2 | 4.32 | 2 | 0.07 | 1 | 7.43 | 5 | 0.09 |
| 1 | 4.50 | 3 | 0.02 | 1 | 7.60 | 4 | 0.03 |
| 2 | 5.27 | 4 | 0.01 | 1 | 7.94 | 2 | 0.01 |
| 1 | 5.60 | 1 | 0.01 | 1 | 7.89 | 6 | 0.01 |
| | | | | 2 | 8.30 | 6 | 0.02 |
| | $Ti^{47}(p,d)Ti^{46}$ | | | 2 | 8.41 | 4 | 0.13 |
| 1 | 1.10 | 2 | 0.61 | 2 | 8.44 | 3 | 0.08 |
| 1 | 2.17 | 4 | 1.74 | 2 | 8.53 | 5 | 0.11 |
| 1 | 2.77 | 2 | 0.18 | 2 | 8.62 | 2 | 0.03 |
| 1 | 3.22 | 4 | 0.03 | 2 | 9.17 | 5 | 0.04 |
| 1 | 3.26 | 6 | 0.15 | 2 | 9.19 | 4 | 0.01 |
| 1 | 3.69 | 2 | 0.04 | 2 | 9.92 | 2 | 0.01 |
| 1 | 3.90 | 4 | 0.47 | 2 | 10.34 | 6 | 0.01 |

| $T$ | $E$ | $I$ | $S$ | $T$ | $E$ | $I$ | $S$ |
|---|---|---|---|---|---|---|---|
| | $Ti^{49}(p,d)Ti^{48}$ | | | | $V^{51}(p,d)V^{50}$ | | |
| 2 | 0 | 0 | 0.25 | 2 | 0 | 6 | 1.14 |
| 2 | 1.22 | 2 | 0.78 | 2 | 0.11 | 4 | 0.27 |
| 2 | 2.02 | 2 | 0.38 | 2 | 0.13 | 3 | 0.39 |
| 2 | 2.52 | 4 | 0.70 | 2 | 0.22 | 5 | 0.53 |
| 2 | 3.01 | 3 | 0.01 | 2 | 0.32 | 2 | 0.46 |
| 2 | 3.35 | 4 | 0.90 | 2 | 0.87 | 5 | 0.64 |
| 2 | 3.36 | 6 | 1.03 | 2 | 0.88 | 4 | 0.67 |
| 2 | 3.49 | 6 | 1.31 | 2 | 1.21 | 7 | 1.69 |
| 2 | 3.83 | 1 | 0.01 | 2 | 1.58 | 1 | 0.14 |
| 2 | 3.97 | 2 | 0.02 | 2 | 1.61 | 2 | 0.06 |
| 2 | 4.35 | 4 | 0.19 | 2 | 2.03 | 6 | 0.11 |
| 2 | 4.58 | 5 | 0.01 | 2 | 2.07 | 3 | 0.25 |
| 2 | 4.97 | 6 | 0.27 | 2 | 2.65 | 7 | 0.08 |
| 2 | 5.14 | 4 | 0.02 | 2 | 2.83 | 3 | 0.13 |
| 2 | 5.30 | 3 | 0.04 | 2 | 2.85 | 2 | 0.01 |
| 2 | 5.50 | 4 | 0.05 | 2 | 2.95 | 1 | 0.07 |
| 2 | 5.55 | 7 | 0.04 | 2 | 3.19 | 5 | 0.08 |
| 2 | 5.91 | 7 | 0.06 | 2 | 3.22 | 3 | 0.07 |
| 2 | 6.07 | 3 | 0.04 | 2 | 3.30 | 6 | 0.08 |
| 2 | 6.25 | 6 | 0.01 | 2 | 3.86 | 7 | 0.05 |
| 2 | 6.61 | 5 | 0.09 | 2 | 4.22 | 1 | 0.17 |
| 2 | 6.95 | 5 | 0.03 | 2 | 4.34 | 6 | 0.11 |
| 2 | 7.01 | 2 | 0.01 | 3 | 4.64 | 0 | 0.13 |
| 2 | 7.02 | 4 | 0.03 | 2 | 4.73 | 2 | 0.03 |
| 2 | 7.16 | 6 | 0.07 | 2 | 4.82 | 5 | 0.12 |
| 2 | 7.20 | 4 | 0.01 | 2 | 5.50 | 3 | 0.03 |
| 2 | 7.29 | 6 | 0.07 | 2 | 5.72 | 4 | 0.05 |
| 2 | 7.76 | 5 | 0.07 | 2 | 5.93 | 7 | 0.05 |
| 2 | 7.82 | 5 | 0.07 | 3 | 6.15 | 2 | 0.07 |
| 2 | 8.27 | 6 | 0.03 | 3 | 6.60 | 5 | 0.01 |
| 2 | 8.29 | 7 | 0.03 | 3 | 7.64 | 4 | 0.12 |
| 2 | 8.51 | 4 | 0.02 | 3 | 8.04 | 6 | 0.18 |
| 2 | 8.40 | 7 | 0.02 | | | | |
| 3 | 10.37 | 6 | 0.10 | | | | |
| 3 | 10.53 | 5 | 0.11 | | | | |
| 3 | 10.83 | 4 | 0.07 | | | | |
| 3 | 10.99 | 3 | 0.03 | | | | |
| 3 | 11.11 | 2 | 0.01 | | | | |
| 3 | 11.72 | 7 | 0.03 | | | | |

## APPENDIX I

Shell-model predictions (Ref. 11) for the energies and spectroscopic factors for $(p,d)$ reactions on stable targets in the $1f_{7/2}$ shell are given in Table VIII. Column 1 lists the isotopic spin, column 2, the predicted energy in MeV, and column 3, the spin of the residual level. Column 4 gives the predicted spectroscopic factor as defined in the text. Levels with predicted spectroscopic factors less than 0.01 are not included.

In certain cases, it is possible to relate the parameter $\beta$ to the two-particle residual interaction. If one has a model wave function $\Phi(\pi, \nu+1)$ for the target nucleus, then one can calculate

$$\delta E=\langle\Phi(\pi, \nu+1)|H_{\pi-1,\nu+1}-H_{\pi,\nu}|\Phi(\pi, \nu+1)\rangle \times\frac{(\nu+1)(\nu+2-\pi)}{(\nu+2)(\nu+1-\pi)}. \quad (22)$$

Here $H_{\pi-1,\nu+1}$ is the Hamiltonian for the $\nu+1$ target neutrons but only $\pi-1$ of the $\pi$ target protons, whereas $H_{\pi,\nu}$ is the Hamiltonian for the $\pi$ target protons but only $\nu$ of the $\nu+1$ target neutrons. If one represents an even-$Z$ target with 28 neutrons by the wave function $\Phi(f_{7/2}{}^{\pi}, I_p=0)\Phi(f_{7/2}{}^{8}, I_n=0)$, then (22) leads to

$$\delta E=(9-\pi)\tfrac{1}{8}(5\epsilon_2-\epsilon_0-4\epsilon_1), \quad (23)$$

where

$$\epsilon_0=\langle f_{7/2}{}^2, I=0|V|f_{7/2}{}^2, I=0\rangle,$$
$$\epsilon_2=(1/27)\textstyle\sum_{I=2,4,6}(2I+1)\langle f_{7/2}{}^2, I|V|f_{7/2}{}^2, I\rangle,$$
$$\epsilon_1=(1/36)\textstyle\sum_{I=1,3,5,7}(2I+1)\langle f_{7/2}{}^2, I|V|f_{7/2}{}^2, I\rangle,$$

and $V$ is the effective interaction between the $f_{7/2}$ nucleons. The two-particle energies used by McCullen, Bayman, and Zamick[11] lead to $\delta E=1.133\ (9-\pi)$, and thus to a $\beta$ of 2.266, in good agreement with the measured values for $_{22}Ti_{27}{}^{49}$, $_{24}Cr_{27}{}^{51}$, and $_{26}Fe_{27}{}^{53}$. The McCullen, Bayman, and Zamick wave function for $Ti^{48}$ leads to a $\delta E$ for $Ti^{47}$ of 6.00 MeV, or $\beta=2.4$. This is somewhat higher than the calculated value for the other three $f_{7/2}$-shell nuclei, in rough agreement with the data.

## ACKNOWLEDGMENTS

The authors are indebted to Dr. B. Bardin and Dr. M. Kondo for their assistance in taking the data, to G. H. McCall and E. R. Martin for their help in data reduction, and to F. Karasek of Argonne National Laboratory for preparation of some of the targets. We wish to thank Dr. R. M. Drisko and Dr. F. G. Perey for making available their Oak Ridge computer programs. We are indebted to Dr. J. B. French, Dr. J. Schiffer, and Dr. E. Kashy for illuminating discussions and to Dr. John D. Anderson for helpful correspondence and for unpublished information on Coulomb energies. One of us (R.S.) wishes to express his appreciation to Professor D. Lind, Professor J. Kraushaar, and Professor R. Smythe of the University of Colorado Nuclear Physics Laboratory for the opportunity to participate in the experimental work.